An Information-Processing Model of the BOLD Response in Symbol Manipulation Tasks

John R. Anderson
Yulin Qin
Myeong-ho Sohn
Cameron Carter

Psychology Department
Carnegie Mellon University
Pittsburgh, PA 15213
(412) 268-2781

ja+@cmu.edu

Monday, January 28, 2002

Abstract

Two imaging studies were performed – one of an algebraic transformation task studied by Anderson, Reder, and Lebiere (1996) and the other of an abstraction symbol manipulation task studied by Blessing and Anderson (1996). ACT-R models exist that carefully model the latency patterns in these tasks. These models require activity of an imaginal buffer to represent changes in the problem representation, in a retrieval buffer to hold information from declarative memory, and in a manual buffer to hold information about motor behavior. A general theory is described about how to map activity in these buffers onto the fMRI bold response. This theory claims that the BOLD response is integrated over the duration a buffer is active and can be used to predict the observed BOLD function. Activity in the imaginal buffer is shown to predict the BOLD response in a left, posterior parietal region; activity in the retrieval buffer is shown to predict the BOLD response in a left DLPFC region; and activity in the manual buffer is shown to predict activity in a motor region.

Cognitive models have been increasingly successful at accounting for complex data sets on problem-solving (Anderson & Lebiere, 1998; Meyer & Kieras, 1997; Pew & Mavor, 1998). Largely, these cognitive models have focused on reaction time and accuracy and usually only final times and accuracies. These models often specify rather complex sequences of unseen processes taking place over many seconds. Even when the pattern of data they fit is correspondingly complex, one is naturally wary about a chain of inferences about unseen processes. It would be better if we could have data about these intervening processes. Basically, more converging data would be better. This paper will demonstrate the potential of functional magnetic resonance imaging (fMRI) data to provide one source of converging evidence. Symmetrically, the paper will show the potential of cognitive models to give a precise explanation of the blood oxygen level dependent (BOLD) response.

The ACT-R theory (Anderson & Lebiere, 1998), particularly in its current 5.0 version, has made itself open to such data. Figure 1 illustrates the basic architecture of that system. The external and internal system interact through a set of cortical buffers that hold information. Particularly important to this paper are the goal buffer, the imaginal buffer, the motor buffer, and the retrieval buffer. The goal buffer keeps track of one's internal intentions in solving a problem. The imaginal buffer essentially keeps a visual image of the problem state – all problem-state representations need not be visual but they are in the algebraic tasks we will be investigating. The manual buffer (Byrne & Anderson, 1998) is used to program hand movements and is based on the EPIC (Meyer &

Kieras, 1997) manual processor. The retrieval buffer requests information from declarative memory and holds the retrieval results. The ACT-R 5.0 specifies when these buffers will be active during the performance of such a task and for how long.

Our main concern in this paper is with the activity of these buffers in ACT-R and their corresponding cortical regions, but we will say a little about how we assume they interact with the rest of the system in Figure 1. In line with other proposals (e.g., Amos 2000; Frank, Loughry, & O'Reilly 2000; Houk & Wise, 1995; Wise, Murray, & Gerfen, 1996) we assume that these cortical areas project to the striatum which serves as a pattern recognition function. The basal ganglia essentially implement production rules in ACT-R which recognize and act on patterns in the cortical areas. Since production rules represent ACT-R's procedural memory this also corresponds to proposals that basal ganglia serve as a procedural memory (Ashby & Waldron, 2000; Hikosaka et. Al, 1999; Saint-Cyr, Taylor, & Lang, 1988). An important function of the production rules is to update the buffers (and there are projections from the thalamus to all of these regions). Thus, the critical cycle in ACT-R is one in which the buffers hold representations determined by the external world and internal modules, patterns in these buffers are recognized and a production fires, and the buffers are then updated for another cycle.

The plan of this paper will be to take tasks for which there already existed well-specified ACT-R models, determine the predictions about module activities, and look for neural correlates. We will describe two experiments based on the research of Anderson, Reder, and Lebiere (1996) and Blessing and Anderson (1996), for which there already exist

ACT-R models. The Anderson, Reder, and Lebiere paper looked at solving of algebraic equations of different complexity and with or without a concurrent memory load. The processes we will propose for their solution do not require any mathematics-specific faculties but general faculties such as for goal maintenance, visual representation or problem state, motor, and declarative retrieval. To confirm that the neural correlates found in this experiment are not specific to mathematical problem solving we looked at the symbol manipulation task of Blessing and Anderson that has removed all of the arithmetic content. It allows a strong converging test of our theory because we can use the regions of interest uncovered in the one study to organize the fMRI data for the other study.

Before describing these experiments, we would like to say a bit about the cortical regions that we expect to see corresponding to the buffers in Figure 1. The goal and the retrieval buffers are rather difficult to separate, both in the behavior of ACT-R and in terms of their localization. Both retrieval operations and goal-setting operations have been associated with the prefrontal cortex. The HERA model (Nyberg, Cabeza, & Tulving, 1996; Tulving, Kapur, Craik, Mosovitch & Houle, 1994) associates episodic and semantic retrieval with right and left prefrontal cortex, respectively. In their recent review, Cabezza and Nyberg (2000) usually found activation in classic prefrontal areas like Brodmann's areas 9, 44, 45 and 46. These same areas also tend to be active in task that involve goal manipulations like task switching (Sohn, Ursu, Anderson, Stenger, & Carter, 2000), Stroop (MacDonald, Cohen, Stenger, & Carter, 2000), and the Wisconsin Card Sorting task (Berman, Ostrem, Randolph, Gold, Goldberg, Coppola, Carson,

Herscovitch, & Weinberger, 1995; Goldberg, Berman, Fleming, Ostrem, Van horn, Esposito, Mattay, Gold, & Weinberger, 1998). In the ACT-R model, goal changes often require retrieval of relevant information. Thus, the predictions for the two buffers are often correlated. We will focus on the behavior of the retrieval buffer, because that is somewhat easier to quantify in ACT-R, leaving open the possibility that effects we attribute to it might be attributed the goal buffer. In any case, the hypothesis is that use of the retrieval buffer will be correlated with activity in prefrontal cortex. Note that the assumption is that the retrieval buffer holds the products of the retrieval, but in line with other proposals the actual memories are stored in other structures.

The visual imagery buffer holds a representation of visual problems during the course of their solution. Given that skilled algebraic manipulation is thought to be highly visual and spatial (Kirsher, 1989; Kirsher & Awtry, submitted) we expect to see changes in the mental state of the equation represented by changes in that buffer. The literature on spatial imagery would associate that with the posterior parietal cortex (Brodmann's areas 7, 39, and 40). In their review, Cabezza and Nyberg note that these regions are active in almost every study of imagery. Reichle, Carpenter, and Just (2000) find greater activation in this area when participants engage in an imagery strategy during language processing and that this is more concentrated in the left parietal regions. Perhaps it is concentrated in the left parietal region because of its connection with the symbolic structure. Since algebra is likewise a meaningful symbol system, our hypothesis is that activation in the left parietal region will track changes in the visual buffer which in turn will reflect changes to the equation representation.

With respect to the manual buffer, it is devoted in ACT-R to representing and monitoring hand movement usually as part of motor programming. It would be natural to associate it with the region of motor cortex that in fact controls the hand. In some sense, including the manual buffer provides us with an anchor point in our interpretation and model fitting since there is good prior localization of the region that is responsible for hand movements. If we can predict its behavior with the same parameters as used for the more cognitive buffers, this will make the association of the cognitive buffers with their areas more secure.

Experiment 1

Table 1 illustrates the 6 conditions of our experiment which were closely modeled on Anderson, Reder, and Lebiere (1986) although some changes were made to meet the methodological demands of the magnet. The equations either required 0, 1 or 2 algebraic transformations to solve. Orthogonal to this, the equations could have two letter constants in them and the participants would have to substitute values they had just learned for these constants. Figure 2 illustrates the basic structure of the fMRI trial. The trial began with 3 seconds for study of assignments for three constants. Then an equation was exposed, which might or might not involve two of these constants, and it remained on for 7.5 seconds. This was followed by a white * for 7.5 seconds to allow the hemodynamic response to settle, followed by a red + for 3 seconds to alert the participant to the next upcoming trial.

Anderson et al. (1996) had found that this task could be understood by tracking its retrieval requirements.[1] There are two types of retrievals, which they found weighted equally in determining accuracy and latency. One type involved arithmetic retrievals which had two subtypes--- retrieving arithmetic facts like 6*3=18 and the other was retrieving information about operator inverses (e.g., - is the opposite of + — a fact that is required to undo a plus operation). The other major type was retrieval of the assignments of values to constants just made (such as b = 5). While ACT-R treats these two retrievals as of the same kind; it was not obvious that they would be so treated by the brain. Indeed, based on the HERA model one might categorize the first as semantic and predict that they would occur in the left prefrontal cortex and the second as episodic and predict that they would occur the right prefrontal cortex.

Method

Task and Procedure

Table 1 shows samples of equations used in this experiment. The participant's task was to solve the equation (i.e., isolate the x), and key in the correct answer. The answers ranged from 6 to 9. Participants used the right index, middle, ring, and the little fingers in a response glove to indicate 6 through 9, respectively.

At the beginning of a trial, a memory set of 3 integers was presented for 3 seconds, which was replaced by an algebra equation. Participants were instructed to rehearse these integers until the equation appeared, because half of the algebra equations would require

substitution of constants with these integers. No additional tasks were required regarding the memory set other than the substitution. The equation itself remained on the screen for 7.5 seconds. If no response was given during this time, the trial was scored as incorrect. The equation then was replaced by an asterisk "*" for 7.5 seconds of rest. Finally, a plus sign "+" appeared for 3 seconds of warning for the next trial.

Parametric design

Two factors were manipulated. First, equations differed in computational complexity. The 0-transformation problems did not require any algebraic transformations. These equations always contained "1" as the slope, and "0" as the constant (e.g., 1x+0=06). Therefore, the answer can be the integer on the right-hand side of the equation. The 1-transformation problems required moving either the constant or the slope to the right-hand side of the equation, but not both. The 2-transformation problems required moving both constant and slope to solve. Rather unusual presentation format of algebra equations that we adopted (such as keeping "1" and "0" for simpler questions) was to keep the visual fields of the stimuli as consistent as possible across different problem complexities.

Second, the integers for an equation were either directly available from the equation (no-substitution) or had to be retrieved from the memory set (substitution). The memory set consisted of three integers. Participants were instructed to treat them as the values for the constant 'a', 'b', and 'c', in left to right order. In the substitution condition, the subsequent equation contained two of these constant letters (e.g., a / x – b = 12), and a

participant had to retrieve the values for these constants to solve the equation. In the no substitution condition, the values were given directly in the equation.

Pre-scan practice

Participants took about 30 minutes of pre-scan practice on the day before the scan day. At first, key-practice program was run to acquaint them with the finger-to-key mapping with a hand-held response glove (press the index finger for 6, the middle finger for 7, the ring finger for 8, and the little finger for 9). Then there were 4 blocks of task practice, 18 trials for each block. The feedback on accuracy and reaction time was given in the end of each trial in the first two blocks. In the last two blocks, no trial-by-trial feedback was given to correspond to the procedure in the scanner.

Event-related fMRI scan

Event-related fMRI data was collected by using a single-shot spiral acquisition on a GE 3T scanner, 1500 ms TR, 18 ms TE, 70^0 flip angle, 20 cm FOV, 3.2 mm thick, 64x64 matrix, 28 slices with AC-PC on the 8^{th} slice from the bottom. There were 14 scans (21 seconds) for each trial, 18 trials for a block and 8 blocks for each participant. There was no trial-by-trial feedback. The protocol of each trial of scan is illustrated in Figure 2.

Images acquired were analyzed using the NIS system.[2] Images first were realigned using 12-parameters AIR (Woods, Grafton, Holmes, Cherry, & Mazziotta, 1998) and then cross-registered to a common reference brain by minimizing signal intensity difference after which functional images were set to a standard mean intensity, smoothed (8mm

FWHM 3D Gaussian kernel) and pooled across subjects to improve signal-to-noise ratio. Spatial F-maps were generated using ANOVA. Regions of interesting (ROIs) were identified by thresholding spatial F-maps of condition (with the requirement of six contiguous voxels, p<=0.01, with df corrected by Greenhouse-Geisser).

Participants

Participants were 8 right handed, native English speakers (4 females). Age ranged from 19 to 23, average 21.5.

Results

Average accuracy was 84.7% and accuracy showed a strong negative correlation with latency (r = -.878). Only correct trials were analyzed. Figure 3 shows the latency results from the experiment. There are large and significant effects of both number of transformations ($F(2, 14) = 260.44$, $p < .0001$; MSE = 81,806) and substitution (($F(1,7) = 135.14$; $p < .0001$, MSE = 154,207) and no interaction between these factors ($F(2\ 14) = .83$; MSE = 74,115). As can be seen these latency effects are consistent with the ACT-R model that we will present.

Analysis of latency and fMRI data was restricted to trials on which the participants were accurate. Regions of interest (ROIs) were selected according to the interaction term in a 6 condition x 14 scans ANOVA. To have a conservative test that dealt with non-independence of scans we used the correction of assigning only 5 degrees of freedom to the numerator in the F-statistic for the interaction term (the Greenhouse-Geisser

correction for non-independence of conditions). The interaction was examined in each voxel, and the selected regions met the criteria of minimum 6 contiguous voxels with significant interaction at p <= .01 (Forman, Cohen, Fitzgerald, Eddy, Minton, & Noll, 1995). Figure 4 and Table 2 give the seven regions which achieve this level of significance. Figure 4 only displays the top 16 slices since there were no significant voxels found lower in the brain. ROIs 1 & 3 are in the posterior parietal cortex and ROI 2 is in the anterior cingulate gyrus. ROI 1 has been found to be active in almost all studies of mathematical thinking (e.g., Dehaene, Spelke, Pinel. Stanescu, & Tsivkin,. 1999; Menon, Rivera, White, Glover, & Reiss, 2000; Zago, Pesenti, Mellet, Crivello, Mazoyer, & Tzourio-Mazoyer, 2001; Gruber, Indefrey, Steinmetz, & Kleinschmidt, 2000; Rickard, Romero, Basso, Wharton, Flitman, & Grafman, 2000). ROI 3 is the precuneous which has also been found active in a number of studies (e.g., Dehaene, et al; Zago, et al). ROI 4 is the left inferior frontal gyrus (BA 44 but above the classic Broca's region) which again has been found in almost all studies of mathematical thinking. ROI 5 is a prefrontal region at the border between Brodman's areas 45 and 46 which has also been found to be active in some studies (Zago, et al.; Gruber, et al.). Regions 6 and 7 are left and right Superamarginal gyrus (Brodman's area 40). Except for ROI 2, which is central, and ROI 6, which is right, the areas of activation are in the left cortex. This is typical of imaging studies of mathematical tasks. Damage in the vicinity of ROI 1, 3 and 7 has also been shown to be associated with acalculia or dyscalulia (Grafman, 1996; Russeli & Ardelia, 1989; Jackson & Warrington, 1986).

Figure 5 shows the activation function for these 7 regions, averaged over condition, as a function of the 14 scans. The dependent measure is percent activation over the baseline set by scan 1. The figure makes the point that the inferior supramarginal ROIs 6 and 7 display somewhat peculiar but similar functions, first falling below zero and then rising above 0. Zago et al (2001) found deactivation in these regions when participants perform calculations. All of the other regions show relatively similar rises and falls. Table 3 shows the intercorrelations between the 7 areas in terms of the 84 observations of the percent change in a conditionxscan analysis. The posterior parietal ROIs 1 and 3 are quite similar with correlations over .9 as are the prefrontal ROIs 4 and 5. While these are the highest intercorrelations, the intercorrelations are positive and fairly strong except for those with ROI 6 and ROI 7, which do not correlate positively with any region except each other. We will focus our analyses on ROI 1 and ROI 5. Both ROI 1 and 3 are from the left posterior parietal region that we expect to be associated with the imaginal buffer in ACT-R. ROI 1 is chosen because it is larger and more reliable but note its high correlation with ROI 3. The 2 prefrontal regions, ROI 4 and ROI 5, also behave similarly. We have chosen to focus on ROI 5 because it is more classic DLPFC. We also chose a third area for investigation, which did not prove to yield a significant interaction in this experiment but did in the next experiment. This is a region that covers the motor and sensory regions corresponding to the right hand. Its exact coordinates will be given as part of Experiment 2 (see ROI 1 in Table 6). The three regions of interest are displayed in Figure 6.

Figure 7 contrasts the behavior of these three regions in the two extreme conditions – no transformation with no substitution versus 2 transformations with substitution. All regions show effects of condition but show different patterns. The posterior parietal and DLPFC particles are quite similar in the most complex condition of 2 transformations with substitution. However, they are dramatically different in the simplest condition of no transformations and no substitution. The posterior parietal particle shows about half the rise as the most complex condition while the DLPFC particle appears to show no effect. As we will see, the DLPFC particle is more sensitive to our complexity manipulation. The motor particle does not show greater magnitude of response in the more complex condition but a greater delay in peaking and a wider distribution – which would be consistent with a later and more variably-timed response.

ACT-R Model

We will now describe the ACT-R model that we developed to fit the behavior profile in Figure 3 and the fMRI functions for these three regions. A complete ACT-R model for performing the experiment and all the conditions is available from web location. It was based on the model in Anderson, Lebiere, and Reder (1996), only being updated from ACT-R 2.0 to ACT-R 5.0. Its two essential aspects are a sequence of transformations of the internal representation of the equation and retrievals. Figure 8 illustrates these for the most complex condition of two transformations with substitution. While there are other things happening involving internal computations, the critical steps involve imaginal transformations, which take 200 msec. each; retrieval operations, which takes an

estimated 600 msec.; and a final motor operation, which takes an 400 msec. Only the retrieval time of 600 msec was estimated to fit the behavioral data. ACT-R has a theory of the microstructure of these retrievals but for current purposes we can treat them as simply taking this fixed time.

The equations have 4 significant symbols that have to be encoded – the term on the right (the c in Figure 8), the first term on the left (the 3 in Figure 8), the operator (the + in Figure 8), and the term before the X (the a in Figure 8). Each time one of these symbols is encoded there is a transformation in the visual image of the equation. The other two symbols (the X and the =) are predictable and are encoded into the equation as part of one of these transformations. In addition, the visual image is transformed if there is a substitution or an algebraic transformation. Thus, depending on condition the number of transformations of the visual image is

$$V = 4 + 2S + A$$

where S = 0 if there are no substitutions and 1 if there are, and A is the number of algebraic transformations.

There are two retrievals required in the case of substitution, one for each algebraic fact retrieved, and 1 to retrieve the inverse of the + or -. (We assume that an inverse operator need not be retrieved in the case of the second operation because it is always divide). Thus the number of retrievals is

R = 2S + 1.5 A

where the 1.5 reflects the fact that two retrievals are required for one of the 1-transformation-condition and only one is required for the other.

Finally, there is always just one motor action and its timing varies with the timing of the response. The fact that there is just a single action may explain why the motor area did not appear as a significant region in this study. It will be significant in the next study where 5 finger presses will be required.

How do the activities of these buffers map into changes in the fMRI signal? A number of researchers (e.g., Boyton et al., 1996; Cohen, 1997; Dale & Buckner, 1997) have proposed that the BOLD response to an event, t time units ago, varies according to the following function:

$$B(t) = t^{a} e^{-t}$$

where estimates of the exponent have varied between 2 and 10. What we propose is that while a buffer is active it is constantly producing a change that will result in a BOLD response according the other above function. The observed fMRI response is integrated over time the buffer is active. Therefore, the observed BOLD response will vary with time as

$$CB(t) = M \int_{0}^{t} i(x) B(\frac{t-x}{s}) dx$$

where *M* is the magnitude scale for response, *s* is the latency scale, and i(x) is 1 if the buffer is occupied at time x and 0 otherwise. Thus, the parameters to be estimated in fitting the BOLD response are *M*, *s*, and *a*. We assume that the scale s and exponent a will be constant across all regions of interest but that the magnitude *M* could differ with region of interest. So, we will estimate a single *s* and *a* and a separate *M* for each regions of interest to produce best fits for the BOLD signal for each of the 6 conditions. Since there are 3 regions of interest, 6 condition, and 14 scans this means we are fitting 3 x 6 x 14 = 252 observations.

There is one complication to our efforts to fit the BOLD responses and this is setting the zero value for each condition. The data in Figures 6 and 7 are graphed as percent change in the BOLD response with respect to scan 1. However, assigning scan 1 as the zero value makes the data particularly subject to any error in the estimate of the BOLD response for that scan. Therefore, we estimated for each condition an ROI offset for scan that yielded best fits to all 14 scans. These constants are subtracted from the percent change BOLD responses for all scans for that condition and ROI. These 18 (6 x 3) corrections tended to be close to zero and amount to lifting or lowering the function a little from what it would be if scan 1 were taken as exactly zero value. These corrections mean that our total parameters are 18 + the 5 theoretically significant parameters. These parameters are reproduced in Table 4. These parameters were estimated by trying to minimize the following quantity:

$$\sum_{i \in ROIs} \sum_{j \in Conditions} \sum_{k \in Scans} (\overline{B}_{ijk} - \hat{B}_{ijk})^2 / s_i^2$$

where $\overline{B}_{ijk}$ is the mean bold response, $\hat{B}_{ijk}$ is the predicted response, and s_i^2 is the mean error in the bold response for ROI *i* calculated by the interaction between the 84 values (6 conditions x 14 scans) by 8 subjects interaction term. Under the hypothesis that all deviations are noise, this quantity is distributed as a chi-square with degrees of freedom equal to the number of observations (252) minus parameters (23)—that is, 229 degrees of freedom. The value of this quantity is 347.86, which is quite significant indicating, not surprisingly, that there are things in the data not predicted by the model. On the other hand, it is not radically different from its expected value of 229 (i.e., the degrees of freedom), indicating that we are capturing most of the systematic variance.

Figures 9-11 reproduce the fits of the model to the data. As can be seen, the actual quality of the fits are generally good with correlations from .972 to .998. The fits to the imaginal buffer activity are particularly good, probability reflecting the large size of the posterior parietal particle and hence very accurate estimate of the means. They clearly capture the relative magnitude of the bold responses in the conditions and this relative magnitude is a parameter-free prediction depending only on the number of transformations. The fits to the DLFPC are quite good and again capture the relative magnitude, which is a parameter-free prediction of number of retrievals. In this case we have a confirmation of Anderson, Reder, and Lebiere's production system model's assumptions about number of retrievals. The fits to the motor region are slightly less

good, reflecting the relatively poor signal-to-noise ratio. Still the prediction is confirmed that the peak of the BOLD response would shift with the time of the response.

Both the DLFPC particle and the Motor particle show some evidence that the BOLD response actually goes below zero and then comes back up. This is the major source of the systematic deviations in the fits of the functions. Glover (1999) has found similar behavior in the motor region and he is able to predict this as the difference of two separately parameterized BOLD functions. We did not want to add such complications to our model for this paper. At the end of the paper we will return to this and other complications that could be added to the mathematical treatment of the BOLD response.

So we have been able to predict three distinct BOLD in three regions from the activity of the ACT-R modules. It is of interest that we can do this with one BOLD function that assumes a common exponent *a* and scale *s* for the three areas. Allowing separate estimates only increases the correlations marginally (for instance, the motor correlations increase by .004). Thus, it seems likely that our fits do reflect some common property of the BOLD response in this experiment.

Experiment 2

Our explanation of the BOLD functions did not depend on the mathematical content of the problems. As noted others have associated left parietal and left prefrontal regions with arithmetic processing.. It would be nice to have confirmation that our chosen areas

did not have anything to do with the mathematical content of these problems. To this end we performed a second experiment that was similar to the previous but removed the arithmetic and number properties of the previous domain. This experiment will also serve as an independent test of the functional assignment of the three areas of interest.

The experiment is adapted from the paradigm of Blessing and Anderson (1996) who were interested in how college students would learn to perform transformations like those in algebra.[3] Our study will not involve as much training as Blessing and Anderson and so our interest will not be in learning but only in the effect of number of transformations. Table 5 illustrates the conditions of our experiment. The participants saw strings that were divided into a left and right side by a <->. On both sides of this symbol were a sequence of symbols which consisted of operators and operands. Operators are encased in circles. The participants' task was to isolate the special symbol P on the left and then type all of the symbols that appeared on the right. In the 0-transformation condition, the string was already in this format and the participants simply had to type the four symbols on the right. In the 1-transformation condition there was an operator on the left before the P, which had to be removed by "undoing". There were 4 operators that had different rules of undoing:

② was undone by switching all ② operators on the right to ③ and vice versa

③ was undone by switching the order of the two operands on the right

④ was undone by switching all ④ operators on the right to ⑤ and vice versa

⑤ could be undone by simply removing it.

The participants had to memorize these four rules for undoing and apply them. In the third condition, 2 transformations, there was also an operator and operand after the P, which had to be removed. There were additional rules for removing these which involved inverting the operator and moving the inverted operator and operand over to the left. The ② and ③ operators were inverses of each other as were the ④ and ⑤ operators. Order of precedence required that these two symbols first be moved over to the right side before the operator before the P was undone.

Note that in all cases there were 4 symbols to be typed in the answer. The subjects were required to complete all transformations in their head before beginning to type the answer. When they had done so and were ready to output the answer they pressed their thumb and then keyed the 4 numbers in the answer with their other fingers. The answers were always some sequence of the digits 2 through 5. They were given 1.5 seconds to key each digit to discourage efforts to compute the answers on the fly. In fact, the time to key the four digits did not vary with condition and only the time for the thumb press varied. The structure of the fMRI trial is illustrated in Figure 12.

Method

Only one factor, the computational complexity, was manipulated in the data analysis of this experiment. The 0-step transformation problems required no symbol arrangement, but simply to copy the answer. The 1-step transformation problems required only

elimination of the operator symbol. The 2-step transformation problems required first moving terms over to the left side and then elimination.

Trial procedure

A trial began with a prompt, which is a column of two rectangles. In the first rectangle, the prompt appeared indicating the complexity of the upcoming problem. After 1.5 seconds, the first rectangle was filled with the problem. Participants were instructed to solve the problem mentally, and press the thumb key when they were ready to key in the final solution, upon which the problem in the first row disappeared. We call the thumb press as the plan time. If the plan time exceeds 18 seconds, the trial was scored as incorrect and the next trial began. After the thumb press, they had 1.5 second to press each of four symbols. The correct answer appeared on the second row as the participants typed in, even when they typed in a wrong answer or missed the 1.5 second response window. Then, a 6 second rest period followed.

Prescan Practice

On the day before the scan, there was a pre-scan session that lasted about 45 minutes. Participants were introduced to new sets of rules, practiced finger-to-key mappings, and practiced actual problem solving. They first practiced 12 problems from the most complex 2-step transformation problems with detailed step-by-step solution, 24 problems of all 3 problem complexities with detailed step-by-step solution, and then 12 more problems from all 3 complexities with no step-by-step solution.

Event-related fMRI scan

The parameters of the event-related fMRI scan were same as in the algebra equation solving experiment. There were 15 blocks in the functional scan with 5 minutes and 30 seconds for each block. We analyzed the first 12 scans starting from the one scan before the presentation of the prompt.

Participants

Group analysis was done from 8 participants' data (right-handed, native English speakers, 3 males/5 females, aged from 18 to 27, average 20.6). The same scanning protocol was used as in the first experiment.

Results

Figure 13 shows the latency results from the experiment. There are large and significant effects of number of transformations ($F(2,14) = 153.12$; $p<.0001$, MSE = 256,156). As can be seen these latency effects are consistent with the ACT-R model that we will present. Overall accuracy was 75.1% and shows a strong negative correlation with latency ($r = -.987$). Again, our analysis of latency and fMRI was restricted to trials where the subject was correct.

Regions of interest were selected according to the interaction term in a 3 conditions x 12 scans ANOVA. The 12 scans consisted of the two 1.5 scans before presentation of the equation and the 10 scans afterwards. To have a conservative test that dealt with non-independence of scans we used that correction of assigning only 2 degrees of freedom to

the numerator in the F statistic for the interaction term. The interaction was examined in each voxel, and the selected regions met the criteria of minimum 6 contiguous voxels with significant interaction at p <= .01. Figure 14 and Table 6 gives the eight regions which achieve this level of significance.[4] Many regions overlap with those found in the first study. ROI 2 in this study is a large bi-lateral posterior parietal regions which includes ROIs 1 and 3 from the previous experiment. ROI 5 in this study is a left DLFPC particle somewhat intermediate between the similarly behaving ROIs 4 and 5 from the previous study. ROIs 6 and 7 in this study correspond to the regions with the same numbering from the previous study. There is no region corresponding to ROI 2 (anterior cingulate) from the previous study. On the other hand, this study has ROI 1 which represents a motor area and ROI 4 which is a polar frontal particle. The are also two small particles, ROIs 3 and 8.

Figure 15 shows the average response to these 8 regions of interest. The parietal (ROIs 2 and 3), prefrontal (ROI 5), motor (ROI 1), and supramarginal (ROIs 6 and 7) regions show similar behavior to that observed in the first experiment. The polar frontal region (ROI 4) shows a large negative response as has been observed in other studies (Gusnard & Raichle, 2001)

To provide consistency with our prior modeling effort we will use the same posterior parietal particle and the DLPFC particle (ROI 5) from the first study along with the motor particle (ROI 1) found in this study. Again they are illustrated in Figure 6. Figure 16 displays the behavior of these three particles as a function of scan and condition. The

figure also contains the predictions of the model that we will describe shortly. The three regions are quite distinct in their behavior. Both the parietal particle and the DLPFC particle show a response that varies with number of transformations. However, the parietal particle shows a substantial response even in the presence of no transformations while the DLPFC particle shows no response in this case. The Motor particle does not show a differential magnitude of response but a differential delay in the response as a function of number of transformations.

Figure 17 illustrates the activity of the ACT-R modules during a solution of one of these equations. The encoding begins with the identification of <-> sign and then the encoding of the symbols to the right of the sign. Then begins the process of encoding the elements to the left of the sign and their elimination in order to isolate the P. This is similar to the process in the previous algebra experiment of encoding the value to the right of the equal sign followed by undoing the operations to the left of the sign in order to isolate the X. In the example in Figure 17, six operations are required to encode the string and an additional two operations to encode the transformation. If there were no transformations there would be 5 encoding operations which is 3 less (one less symbol in the screen and two fewer symbols to change). If there were two transformations there would be 10 operations because two additional symbols that have to be changed. With respect to retrievals it is necessary to retrieve two pieces of information for each transformation that must be performed. One piece was the operation to perform ("flip" in Figure 17) and the other the identity of the terms to apply this operation to (arguments in Figure 17). Thus, there are 5, 8, or 10 visual operations, and 0, 2, or 4 retrieval operations. In all cases

there are the final 5 motor operations but their timing will vary with how long the overall process takes. The first motor action takes .4 seconds but because of features saved in programming subsequent finger presses, the remaining actions take .3 seconds.

To make the fits from the two experiments comparable, we constrained the scale (s) and exponent (a) parameters to be the same as estimated in the previous experiment. This means that the shape of the underlying BOLD function will be the same in the two experiments. Thus, the estimated parameters are the magnitude and offset parameters for each condition. As Table 4 reveals, the magnitude parameters are similar but somewhat smaller in this experiment. The degrees of freedom are the 108 observations (13 regions x 3 conditions x 12 scans) minus the 12 parameters or 96. The chi-square deviation was 204.73, which is significant and once again indicates are fit is only approximate. Nonetheless, as can be seen from Figure 16 the model does a good job in accounting for the behavior of the three regions. In this experiment with the five finger movements the behavior in the motor region is particularly clear and well fit by the model. The fit to the DLPFC particle may be again suffering from the failure of the current BOLD function to predict an undershoot in the end of the BOLD response The prediction for the DLPFC particle in the 0-transformation condition is particularly dramatic--a flat function because there are no retrievals. While the actual data may show the slightest of rises and undershoots, they provide a close approximation to this strong parameter-free prediction.

Conclusions

First, we would like to begin with some discussion of the approximations in our mathematical treatment. As already noted, we assume the same BOLD function for each region (except for the multiplicative magnitude, M) whereas it is plausible the function might vary a little. Also, we ignore the potential undershoot as the function goes back to baseline. Another issue is the fact that we have ignored the variability in the timing of responses between and within subjects and the model assumes a single mean time for the processing in each condition. The consequence of this approximation perhaps shows up most clearly in Figure 16c where the longer and more variable conditions resulted in a lower and wider BOLD response. We think that all of these approximations are more than justified by the greater simplicity and interpretability of the resulting model. We do not think they at all compromise the basic conclusions. It is also probably the case that our offset parameters somewhat correct for these approximations.

A more fundamental issue has to do with the assumption that the BOLD response increases linearly with the length of an event and is additive across multiple events. While there is evidence for this as an approximate characterization in some situations (e.g., Boyton, 1996; Dale & Buckner, 1997) it does not seem to be universally the case (e.g., Glover, 1999) with evidence for sublinear growth with duration and sub-additivity across events. This could potentially seriously compromise the logic of this and related research in a way that we could not recover from without a basis for characterizing the non-linearities and non-additivities. It remains an open issue just how serious a matter this is, but in our mind it is the major question about the modeling methodology in this paper.

As an empirical summary, this research is largely consistent with existing associations in the literature of parietal cortex with visual and imaginal processing, the prefrontal cortex with retrieval, and the region of somatosensory cortex that represents the right hand with the manual buffer. Each of these associations deserves a little comment. First, while there was bilateral activation of the parietal cortex it was stronger in the left, consistent with other research on arithmetic and imagery processing in language. This is perhaps consistent with the semantic and somewhat abstract nature of the task. Perhaps why the activation was more bilateral in the second study was that we had removed much of the semantic associations and made it a more pure visual task.

Second, our retrieval focus was found in left BA 45/46. Left prefrontal cortex has been associated with semantic retrieval. However, much of what participants in our experiment were retrieving was not classic semantic information. The algebra knowledge and arithmetic knowledge in the first study would seem classic semantic. However, we also found an effect of retrieval of just-memorized constant values in Experiment 1 and of algebraic transformations just learned in Experiment 2. While our retrievals are not semantic in the sense of having been long-learned they are semantic in the sense of being decontextualized knowledge. It is also the case that our region is anterior to the area 44 that seems to have most been found in previous studies of semantic retrieval. We did find very similar activation is high BA 44 (not classic Brocas) which was strongly correlated with the activity in BA 45/46. However, we focused on BA 45/46 in part because it was more strongly related to number of transformations, showing no rise at all

when there was no retrievals required. Interesting, episodic retrieval more often appears to activate right BA 46 than right BA 44.

Finally, we should comment on the fact that our manual buffer was associated with activation in the somatosensory area corresponding to the right hand as well as the motor area. In fact, the motor ROI is very similar to the region identified by Roland et al (1980) when a finger is pressed. It was said (Kolb & Wilshaw, 1990) that in descending motor pathway (Pyramidal tract) for voluntary movement, there are about 1,000,000 fibres, in which 60% come from precentral (BA 4, 6) and 40% come from post central areas (BA 3a, 5).

This paper is built around a tentative mapping from ACT-R buffers to the BOLD response. Undoubtedly, this mapping will have to be revised with further evidence. However, we think the most important contribution of this paper is the conception it offers of how the detailed processing of an information-processing theory like ACT-R can make precise predictions about the BOLD response. We would hope that this conception would survive any revisions in ACT-R and its mapping to brain function. Indeed, we would hope that this same conception can be incorporated by other information-processing theories.

The basic idea is that the BOLD response reflects the duration for which various cognitive modules are active. The typical additive-factors information-processing methodology has studied how manipulations of various cognitive components affect a

single aggregate behavioral measure like total time. If we can assign these different components to different regions we have essentially a separate dependent measure to track each component. Therefore, this methodology promises to offer strong guidance in the development of an information-processing theory.

Finally, we want to comment on the surprising match of fMRI methodology to the study of complex tasks. A problem with fMRI is its poor temporal resolution. However, as is particularly apparent in the behavior of our manual buffer, the typical effect size in a complex mental task is such that one can still make temporal discriminations in fMRI data. One might have thought the outcome of such a complex task would be purely uninterpretable. However, with the guidance of strong information-processing model and well-trained participants one can not only interpret but predict the BOLD response in various regions of the brain.

References

Amos, A. (2000). A computational model of information processing in the frontal cortex and basal ganglia. Journal of Cognitive Neuroscience, 12, 505-519.

Anderson, J. R. & Lebiere, C. (1998). The atomic components of thought. Mahwah, NJ: Erlbaum.

Anderson, J. R., Reder, L. M. & Lebiere, C. (1996). Working memory: Activation limitations on retrieval. *Cognitive Psychology, 30,* 221-256.

Ashby, F. G. & Waldron, E. M. (2000). The neuropsychological bases of category learning. Current Directions in Psychological Science, 9, 10-14.

Blessing, S. & Anderson, J. R. (1996). How people learn to skip steps. Journal of Experimental Psychology: Learning, Memory and Cognition, 22, 576-598.

Berman, K. F., Ostrem, J. L., Randolph, C., Gold, J. Goldberg, T. E. Coppola, R., Carson, R. E., Herscovitch, P., & Weinberger, D. R. (1995). Physiological activation of a cortical network during performance of the Wisconsin Card Sorting Test: A positron emission tomography study. Neuropsychologia, 33, 1027-1046.

Boyton, G. M., Engel, S. A., Glover, G. H., & Heeger, D. J. (1996). Linear systems analysis of functional magnetic resonance imaging in human V1. Journal of Neuroscience, 16, 4207-4221.

Byrne, M. D. & Anderson, J. R. (1998). Perception and action. In J. R. Anderson & C. Lebiere (Eds.) The atomic components of thought, 167-200. Mahwah, NJ: Erlbaum.

Cabezza, R. & Nyberg, L. (2000). Imaging Cognition II: An empirical review of 275 PET and fMRI studies. Journal of Cognitive Neuroscience, 12, 1-47.

Cohen, M. S. (1997). Parametric analysis of fMRI data using linear systems methods. NeuroImage, 6, 93-103.

Dale, A. M., Buckner, R. L. (1997) Selective Averaging of Rapidly Presented Individual Trials Using fMRI. Human Brain Mapping, 5, 329-340.

Dehaene, S., Spelke, E., Pinel. P., Stanescu, R. Tsivkin, S. (1999). Sources of mathematical thinking: Behavior and brain-imaging evidence. Science, 284, 970-974.

Forman, S. D., Cohen, J. D., Fitzgerald, M., Eddy, W. F., Mintun, M. A., & Noll, D. C. (1995). Improved assessment of significant activation in functional magnetic resonance imaging (fMRI): use of a cluster-size threshold. Magnetic Resonance Imaging--method., 33, 636-647.

Frank, M. J., Loughry, B. & O'Reilly, R. C. (2000). Interactions between frontal cortex and basal ganglia in working memory: A computational model. Institute of Cognitive Science, University Colorado, Boulder, Technical Report 00-01.

Glover, G. H. (1999). Deconvolution of impulse response in event-related BOLD fMRI. NeuroImage, 9, 416-429.

Goldberg, T. E., Berman, K. F., Fleming, K., Ostrem, J., Van horn, J. D., Esposito, G., Mattay, V. S., Gold J. M., & Weinberger, D. R. (1998). Uncoupling cognitive workload and prefrontal cortical physiology: A PET rCBF study. NeuroImage, 7, 296-303.

Grafman, J., & Rickard, T. C. (1996). Acalculia. In T. E. Fineberg, M. J. Farah (Eds.) Behavioral neurology and neuropsychology. New York: McGraw-Hill.

Gruber, O., Indefrey, P., Steinmetz, H., & Kleinschmidt, A. (2000). Dissociating neural correlates of cognitive components in mental calculation. Cerebral Cortex, 11, 350-359.

Hikosaka, O., Nakahara, H., Rand, M. K., Sakai, K., Lu, Z., Nakamura, K., Miyachi, S. & Doya, K. (1999). Parallel neural networks for learning sequential procedures. Trends in Neuroscience, 22, 10 (256), 464-471.

Houk, J. C. & Wise, S. P. (1995). Distributed modular architectures linking basal ganglia, cerebellum, and cerebral cortex: Their role in planning and controlling action. Cerebral Cortex, 2, 95-110.

Jackson, M. & Warrington, E. K. (1986). Arithmetic skills in patients with unilateral cerebral lesions. Cortex, 22, 610-620.

Kirshner, D. (1989). The visual syntax of algebra. Journal for Research in Mathematics Education, 20, 274-287.

Kirshner, D. & Awtry, T. (submitted). The visual salience of algebra transformational rules. Journal for Research in Mathematics Education.

Kolb, B. & Wilshaw, I. (1990). Fundamentals of human neuropsychology, Third Edition. Need publisher.

MacDonald, A. W., III, Cohen, J. D., Stenger, V. A. & Carter, C. (2000). Dissociating the role of dorsolateral prefrontal and anterior cingulate cortex in cognitive control. Science, 288, 1835-1838.

Meyer, D. E. & Kieras, D. E. (1997a). A computational theory of executive cognitive processes and multiple-task performance. Part 1. Basic mechanisms. Psychological Review, 104, 2-65.

Menon, V., Rivera, S. M., White, C. D., Glover, G. H., & Reiss, A. L., (2000). Dissociating prefrontal and parietal cortex activation during arithmetic processing. NeuroImage 12, 357-365.

Meyer, D. E. & Kieras, D. E. (1997b). A computational theory of executive cognitive processes and multiple-task performance. Part 2. Accounts of psychological refractory-period phenomena. Psychological Review, 104, 749-791.

Nyberg, L., Cabezza, R. & Tulving, E. (1996). PET studies of encoding and retrieval: The HERA model. Psychonomic Bulletin and Review, 3, 135-148.

Pew, R. W., & Mavor, A. S. (1998). Modeling human and organizational behavior: Application to military simulations. Washington, DC: National Academy Press.

Rickard, T. C., Romero, S. G., Basso, G., Wharton, C. M., Flitman, S., & Grafman, J. (2000). The calculating brain: an fMRI study. Neuropsychologia, 38, 325-335.

Rosselli, M., & Ardila, A. (1989). Calculation deficits in patients with right and left hemisphere damage. Neuropsychologica, 27, 607-617.

Saint-Cyr, J. A., Taylor, A. E., & Lang, A. E. (1988). Procedural learning and neostriatal dysfunction in man. Brain, 111, 941-959.

Sohn, M-H., Ursu, S., Anderson, J. R., Stenger, V. A. & Carter, C. (2000). The role of prefrontal cortex and posterior parietal cortex in task switching. Proceeding of the National Academy of Science USA, 97, 13448-13453.

Tulving, E., Kapur, S., Craik, F. I. M., Mosovitch, M., & Houle, S. (1994). Hemispheric encoding/retrieval asymmetry in episodic memory: Positron emission tomography findings. Proceeding of the National Academy of Science USA, 91, 2012-2015.

Wise, S. P., Murray, E. A., & Gerfen, C. R. (1996). The frontal cortex-basal ganglia system in primates. Critical Reviews in Neurobiology, 10, 317-356.

Woods, R. P., Grafton, S. T., Holmes, C. J., Cherry, S. R., & Mazziotta, J. C. (1998). Automated image registration: I. General methods and intrasubject, intramodality validation. Journal of Computer Assisted Tomography. 22, 139.

Zago, L., Pesenti, M., Mellet, E., Crivello, F., Mazoyer, B., & Tzourio-Mazoyer, N. (2001). Neural correlates of simple and complex mental calculation. NeuroImage, 13, 314-327.

Acknowledgements

John R. Anderson, Department of Psychology, Carnegie Mellon University, Pittsburgh, PA 15213 (412) 268-2788, ja+@cmu.edu. This research was supported by the NSF ROLE grant REC-0087396 to Anderson and Carter. We would like to _____ for their comments on an earlier draft of this paper. Correspondence concerning this article should be addressed to John R. Anderson, Department of Psychology, Carnegie Mellon University, Pittsburgh, PA 15213. Electronic mail may be sent to ja+@cmu.edu.

Table 1

Example of the Materials in the Algebra Experiment

Extension of Anderson, Reder, & Lebiere (1996)

	No Substitution	**Substitution**
0 Transformations	1x + 0 = 06	ax + 0 = c (a = 1; c = 6)
1 Transformations	2x + 0 = 12 or 1x + 9 = 18	ax + 0 = c (a = 2; c = 12)
2 Transformations	3x+5 = 23	ax + b = 23 (a = 3; c = 5)

Table 2

Regions of Interest, location of centroids, and significance for Experiment 1

Region of Interest	BA	Voxel Count	Stereotaxic Coordinates (mm)			Maximum F (Average F)
			x	y	z	
1. Left Posterior Parietal	39,40	190	-30	-55	38	5.50 (4.09)
2. Anterior Cingulate	32	32	1	15	39	4.56 (3.98)
3. Left Precuneus	7	10	-2	-66	45	4.27 (3.98)
4. Left Inferior Frontal Gyrus	44	62	-43	4	23	5.19 (4.19)
5 Left Dorsolateral Prefrontal	45/46	29	-42	28	18	4.78 (4.02)
6. Right Supramarginal Gyrus	40	33	58	-18	22	4.13 (3.81)
7. Left Supramarginal Gyrus	40	36	-51	-20	19	4.41 (3.86)

Table 3
Intercorrelations among the activation functions in the various Regions of Interest Identified in Experiment 1

	Roi 2	Roi 3	Roi 4	Roi 5	Roi 6	Roi 7
Roi 1	0.824	0.918	0.814	0.703	-0.364	0.201
Roi 2		0.686	0.609	0.404	-0.325	-0.008
Roi 3			0.632	0.600	-0.207	0.304
Roi 4				0.908	-0.536	0.0508
Roi 5					-0.551	0.0495
Roi 6						0.699

Table 4 Parameters estimated for Experiment 1 & 2

(a) Experiment 1

	Visual Imaginal	Retrieval	Manual
Scale (s)	1.383	1.383	1.383
Exponent (a)	3.670	3.670	3.670
Magnitude (M)	0.219	0.074	0.330
Scan 1 Offsets			
No sub, 0 Trans	0.044	-0.113	-0.037
No sub, 2 Trans	-0.001	-0.061	-0.082
No sub, 1 Trans	-0.021	0.030	-0.040
No sub, 0 Trans	0.038	-0.034	-0.056
No sub, 2 Trans	-0.011	0.042	-0.097
No sub, 1 Trans	0.003	0.042	-0.092

(b) Experiment 2

	Visual Imaginal	Retrieval	Manual
scale (s)	1.383	1.383	1.383
exponent (a)	3.670	3.670	3.670
magnitude (M)	.0127	0.055	0.240
Scan 1 Offsets			
O Trans	0.011	-0.049	0.014
1 Trans	0.030	-0.035	-0.006
2 Trans	0.050	-0.023	-0.052

Table 5
Symbolic Reasoning Experiment
Based on Blessing & Anderson (1996)

Example of equations:

step	equation	answer
0 step	**P** <-> ❸4 ❷5	**P** <-> ❸4 ❷5
1 step	❷**P** <-> ❸4 ❷5	**P** <-> ❷4 ❸5
2 step	❷**P** ❸4 <-> ❷5	**P** <-> ❸5 ❸4

Table 6
Regions of Interest, location of centroid, and significance for Experiment 2

Region of Interest	BA	Voxel Count	Stereotaxic Coordinates (mm)			Maximum F (Average F)
			x	y	z	
1. Left Motor	1-4	290	-40	-24	49	16.10 (9.56)
2. Bilateral Posterior Parietal	39,40	710	-2	-66	36	26.75 (8.59)
3. Left Posterior Parietal	40	6	-33	-49	43	6.95 (6.70)
4. Polar Frontal	10	191	-2	55	19	10.50 (7.84)
5 Left Dorsolateral Prefrontal	46/9	31	-45	21	26	8.87 (7.43)
6. Right Supramarginal Gyrus	40	25	63	-26	26	9.44 (7.46)
7. Left Supramarginal Gyrus	40	28	-54	-24	19	10.55 (7.69)
8. Right Lingual Gyrus	19	11	13	-54	2	7.42(6.84)

Figure Captions

Figure 1 A representation of the information flow in ACT-R 5.0.

Figure 2 The 21 second structure of an fMRI trial in Experiment 1.

Figure 3 Mean latency in Experiment 1 as a function of number of transformations for the substitution and the No Substitution condition.

Figure 4 Activation map showing areas in Experiment 1 with a significant interaction between scan and condition. Only regions with more the 6 contiguous voxels and $p<.01$ are shown. See Table 2 for identification of regions.

Figure 5 Average activation functions for the seven regions of interest from Experiment 1.

Figure 6 An illustration of the three left ROI's for modeling.

Figure 7 Contrasting behavior of the three focus regions in the two most extreme conditions of the experiment.

Figure 8 Buffer activity for the ACT-R model of Experiment 1.

Figure 9 Ability of the imagery buffer to predict posterior parietal particle: (a) effects of number of transformations and (b) effects of substitution.

Figure 10 Ability of Retrieval Buffer to predict DLPFC particle: (a) effects of number of transformations and (b) effects of substitution.

Figure 11 Ability of Manual Buffer to predict Motor particle: (a) effects of number of transformations and (b) effects of substitution.

Figure 12 18 second structure of an fMRI trial in Experiment 2

Figure 13 Mean latency in Experiment 2 as a function of the number of transformations.

Figure 14 Activation map showing areas in Experiment 2 with a significant interaction between scan and condition. Only regions with more the 6 contiguous voxels and $p<.01$ are shown. Slice 18 is the AC-PC line. See Table 6 for identification of regions.

Figure 15 Average activation functions for the eight regions of interest from Experiment 2.

Figure 16 BOLD response in Experiment 2 as a function of scan for 0, 1, and 2 transformations: (a) Posterior Parietal particle, (b) DLPFC particle, and (c) Motor particles. ACT-R predictions are in BOLD.

Figure 17 Buffer activity in the ACT-R model for Experiment 2.

Figure 1

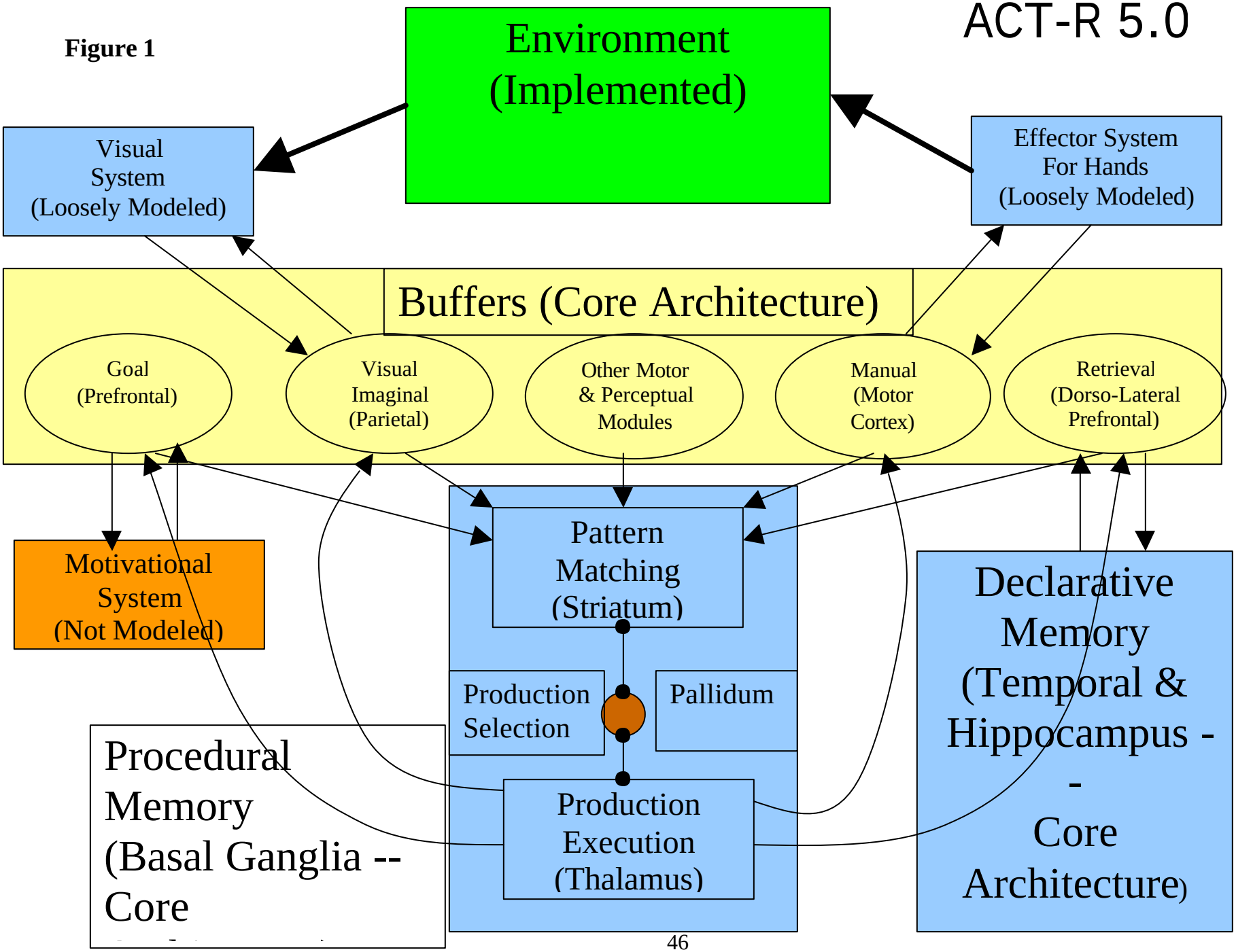
ACT-R 5.0
Environment (Implemented)
Visual System (Loosely Modeled)
Effector System For Hands (Loosely Modeled)
Buffers (Core Architecture)
Goal (Prefrontal)
Visual Imaginal (Parietal)
Other Motor & Perceptual Modules
Manual (Motor Cortex)
Retrieval (Dorso-Lateral Prefrontal)
Motivational System (Not Modeled)
Pattern Matching (Striatum)
Production Selection
Pallidum
Production Execution (Thalamus)
Procedural Memory (Basal Ganglia -- Core
Declarative Memory (Temporal & Hippocampus -- Core Architecture)

Figure 2

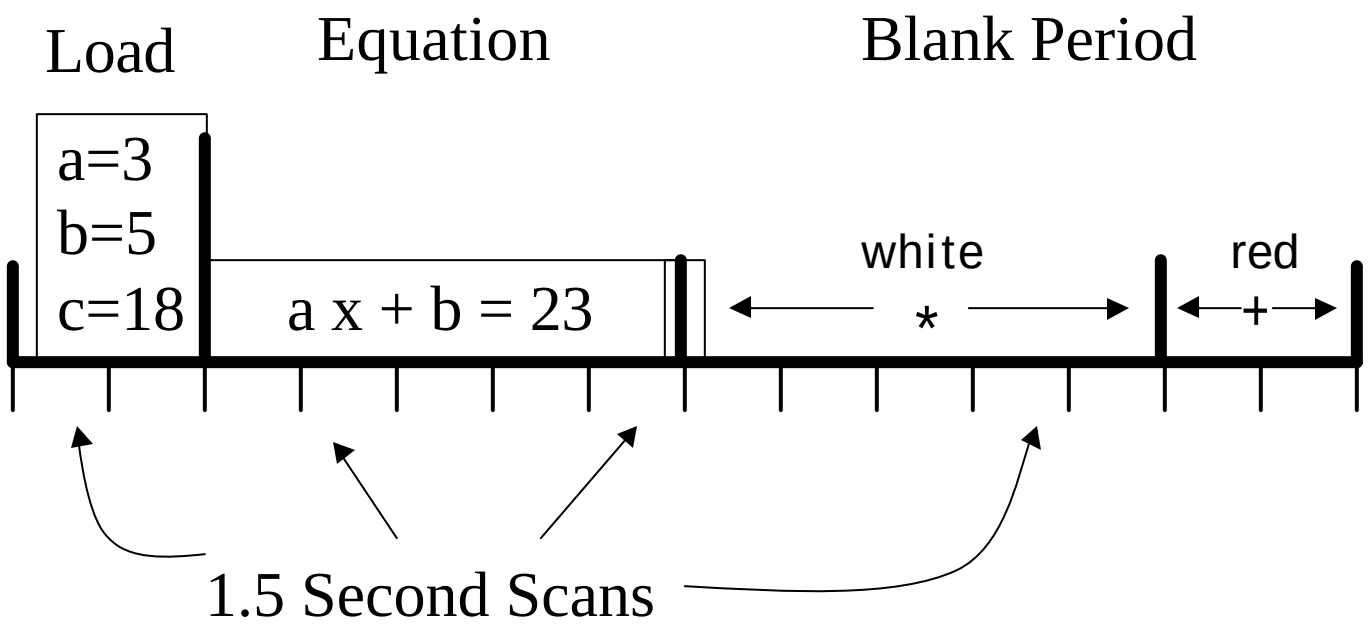
Load
Equation
Blank Period
a=3
b=5
c=18
a x + b = 23
white
*
red
+
1.5 Second Scans

Figure 3

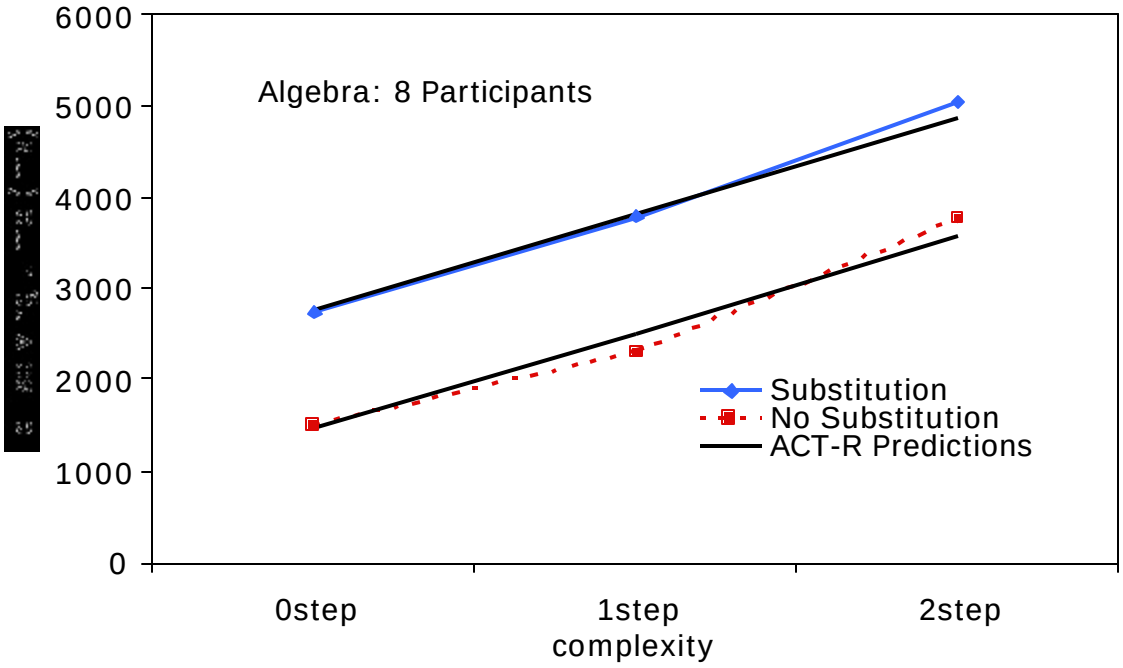
Algebra: 8 Participants
6000
5000
4000
3000
2000
1000
0
0step
1step
2step
complexity
Substitution
No Substitution
ACT-R Predictions

Figure 4

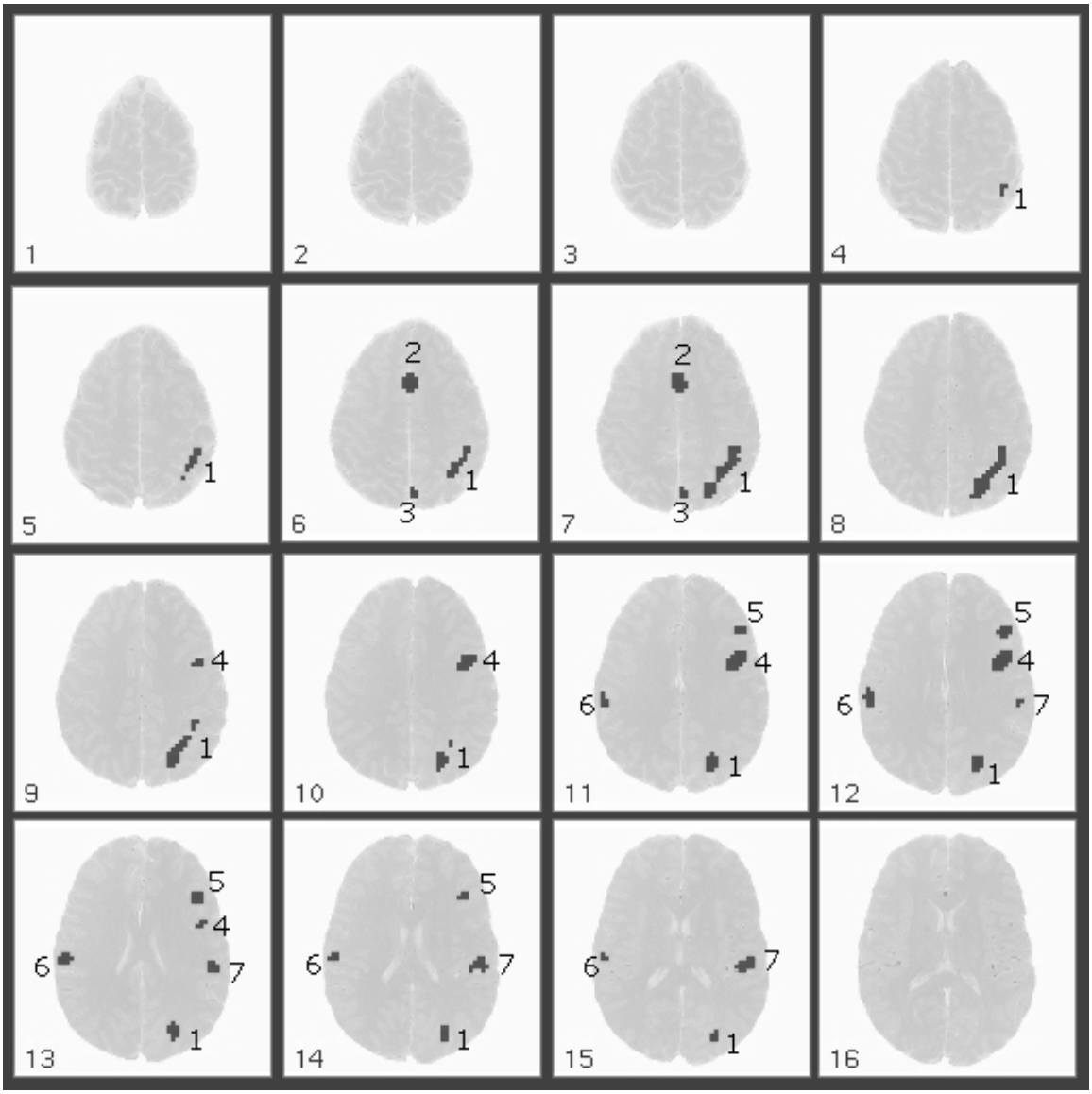
1
2
3
4
1
5
1
6
2
1
3
7
2
1
3
8
1
9
4
1
10
4
1
11
5
4
6
1
12
5
4
6
7
1
13
5
4
6
7
1
14
5
6
7
1
15
6
7
1
16

Figure 5

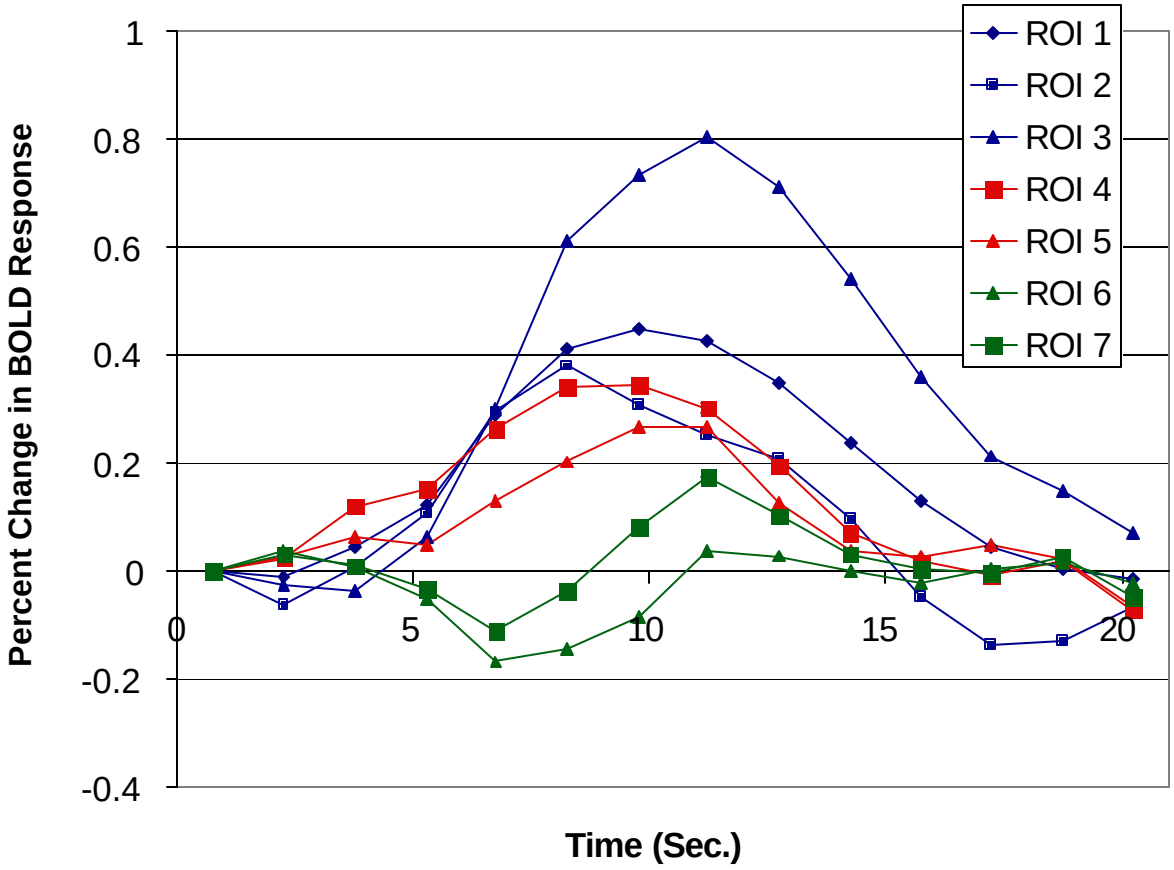
Percent Change in BOLD Response
1
0.8
0.6
0.4
0.2
0
-0.2
-0.4
0
5
10
15
20
Time (Sec.)
ROI 1
ROI 2
ROI 3
ROI 4
ROI 5
ROI 6
ROI 7

Figure 6

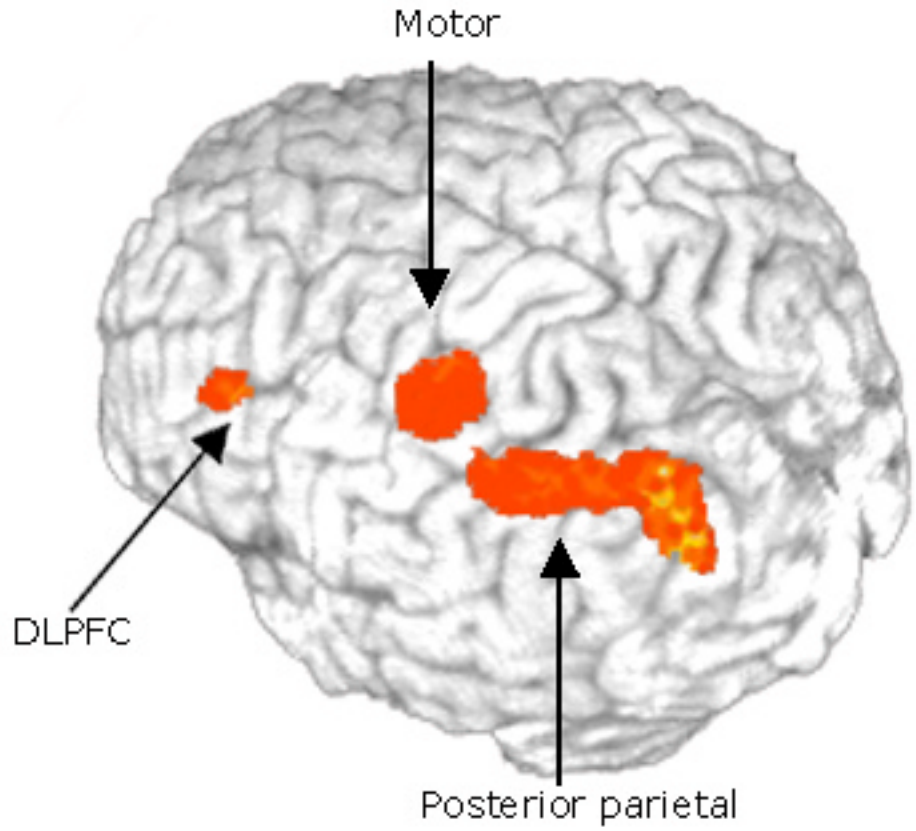

Figure 7

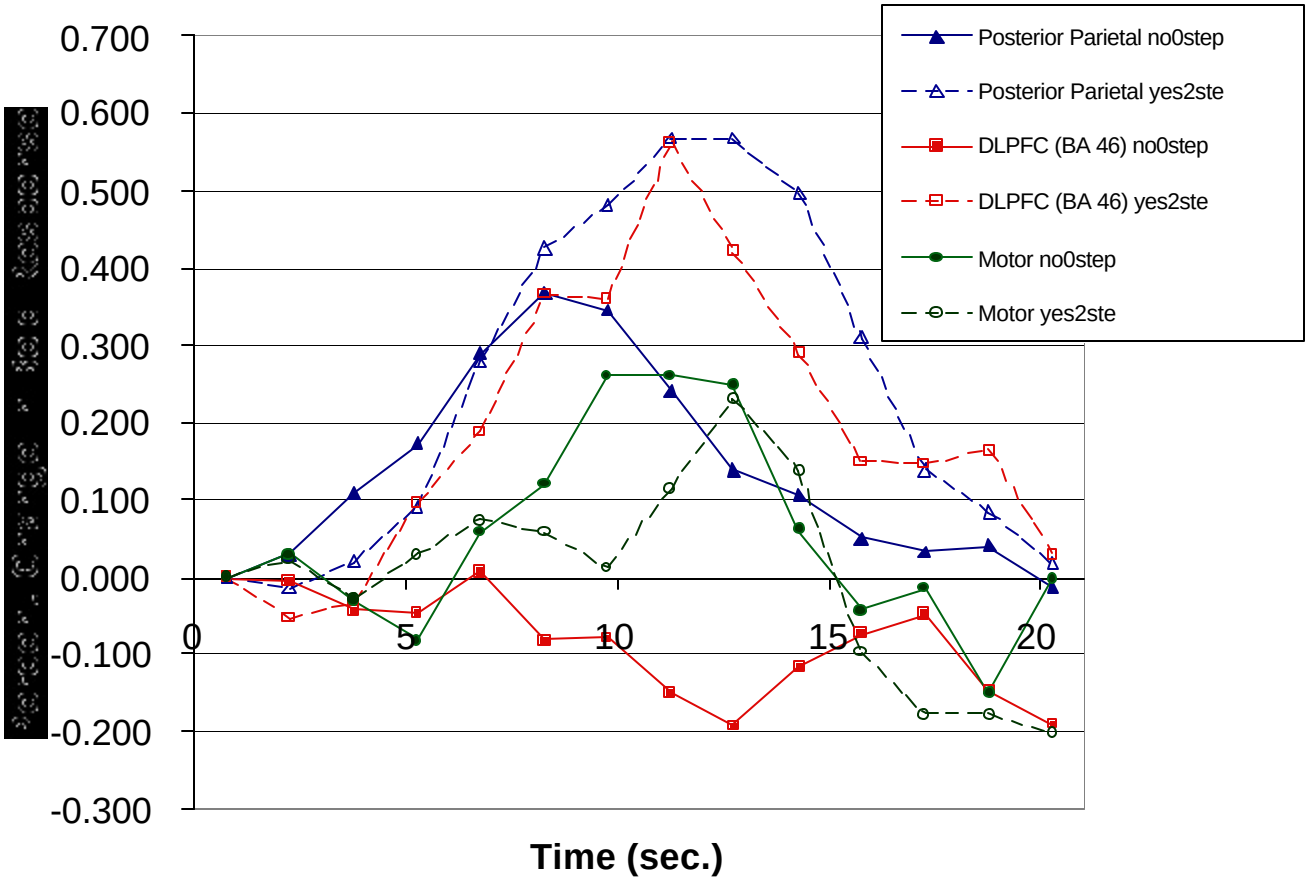
0.700
0.600
0.500
0.400
0.300
0.200
0.100
0.000
-0.100
-0.200
-0.300
0
5
10
15
20
Time (sec.)
Posterior Parietal no0step
Posterior Parietal yes2ste
DLPFC (BA 46) no0step
DLPFC (BA 46) yes2ste
Motor no0step
Motor yes2ste

Figure 8

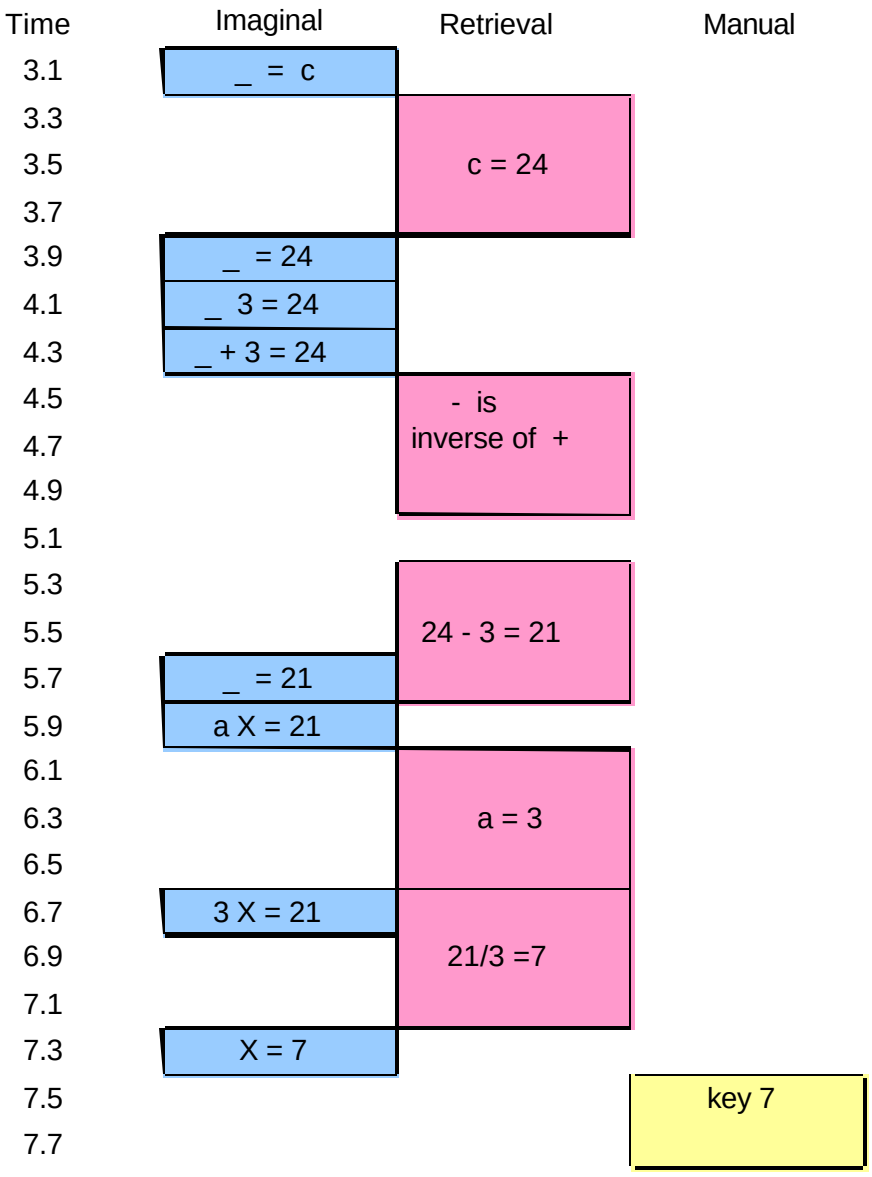
Time
Imaginal
Retrieval
Manual
3.1
3.3
3.5
3.7
3.9
4.1
4.3
4.5
4.7
4.9
5.1
5.3
5.5
5.7
5.9
6.1
6.3
6.5
6.7
6.9
7.1
7.3
7.5
7.7
_ = c
c = 24
_ = 24
_ 3 = 24
_ + 3 = 24
- is inverse of +
24 - 3 = 21
_ = 21
a X = 21
a = 3
3 X = 21
21/3 =7
X = 7
key 7

Figure 9a

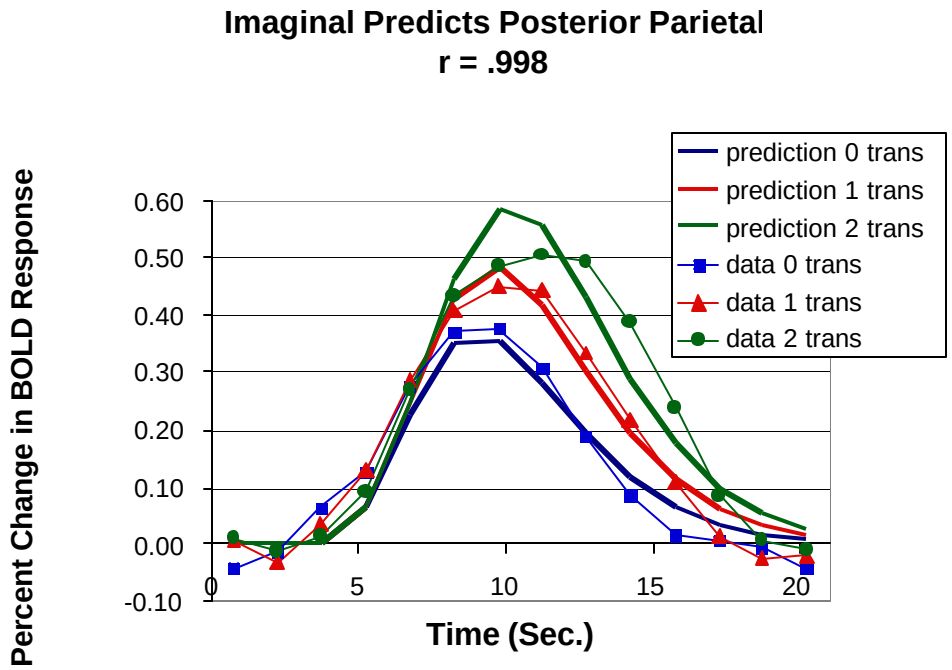

Figure 9b

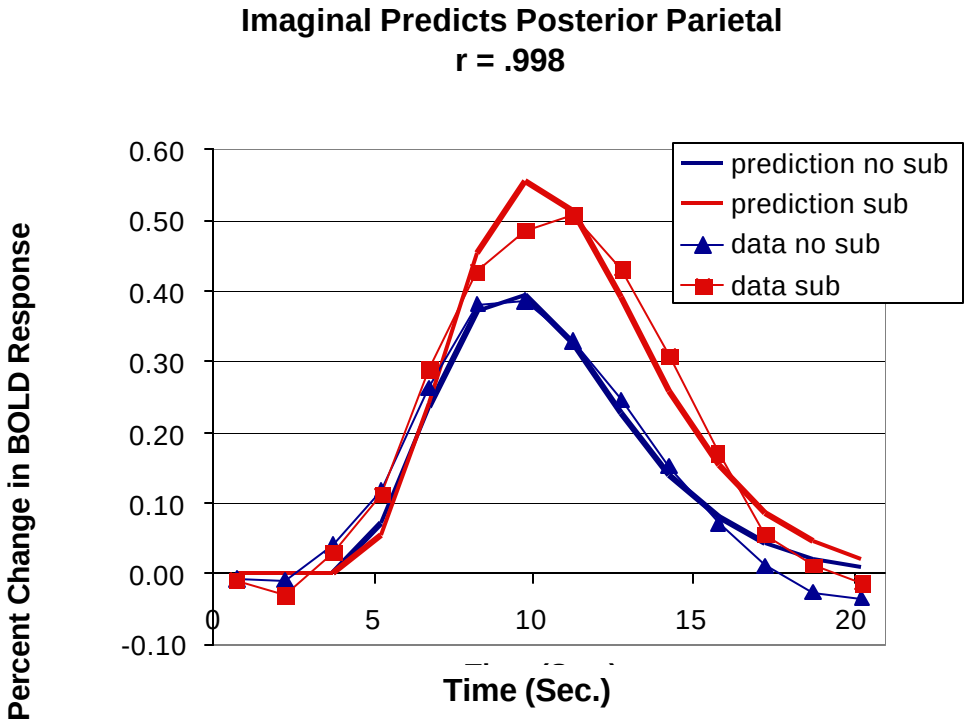

Figure 10a

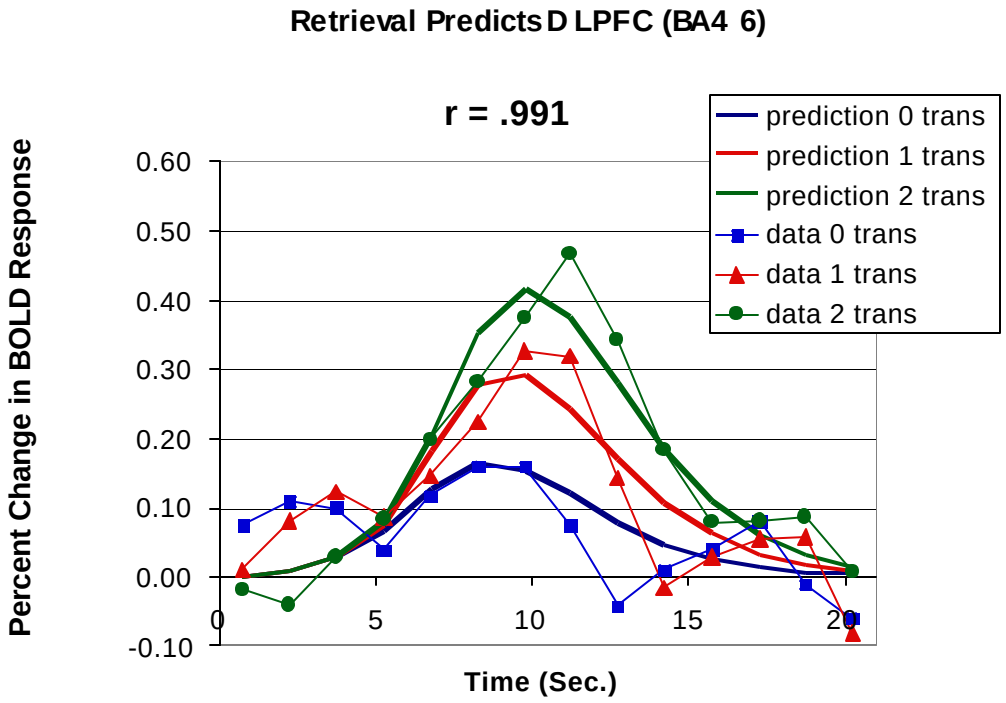

Figure 10b

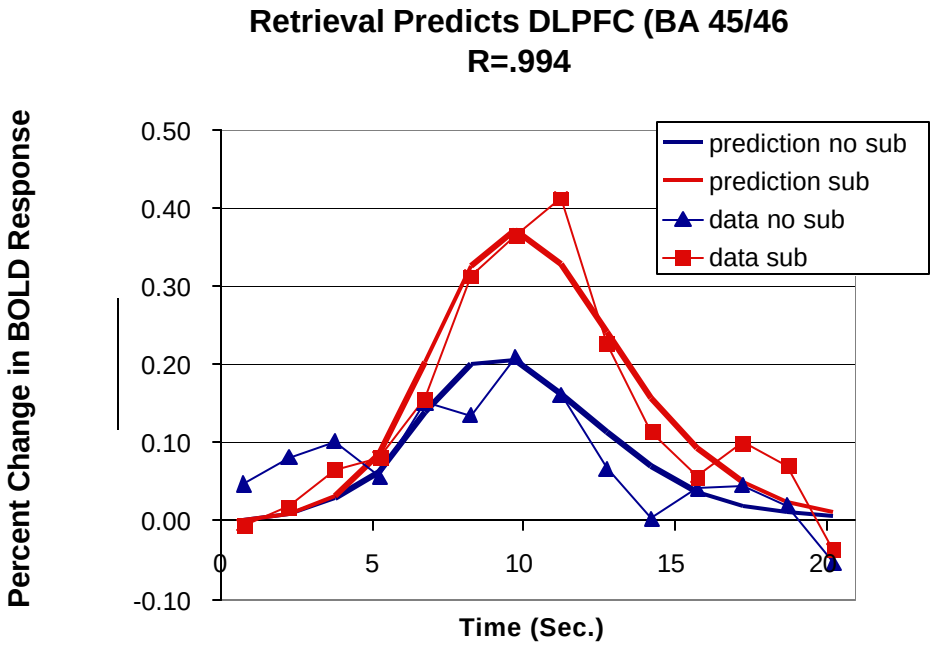

Figure 11a

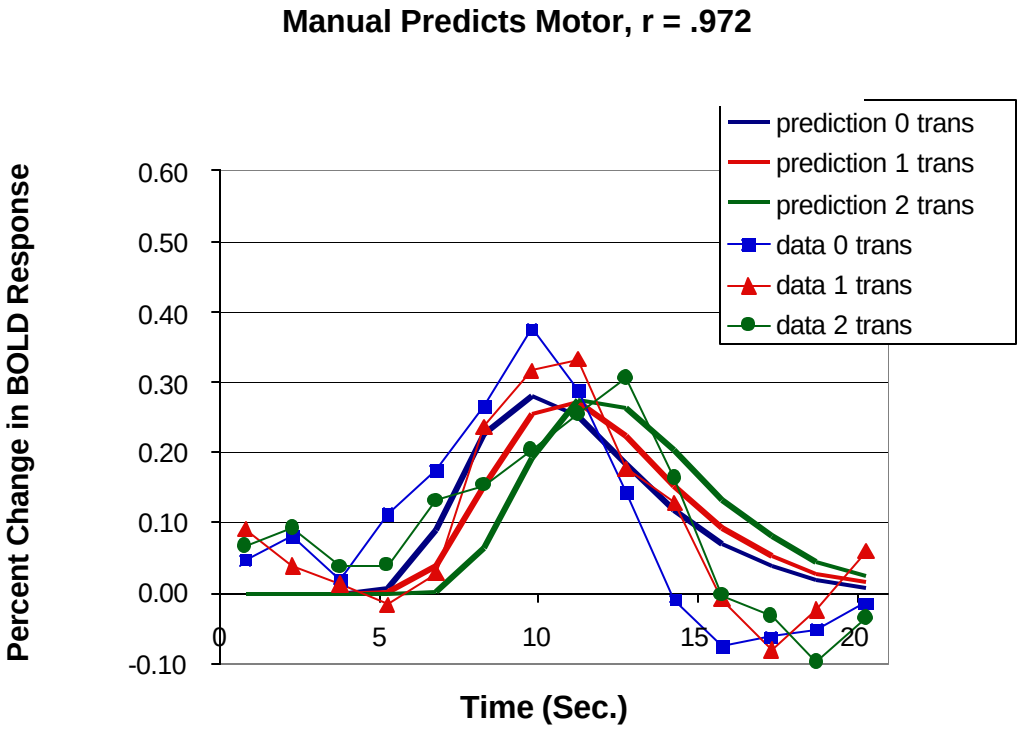

Figure 11b

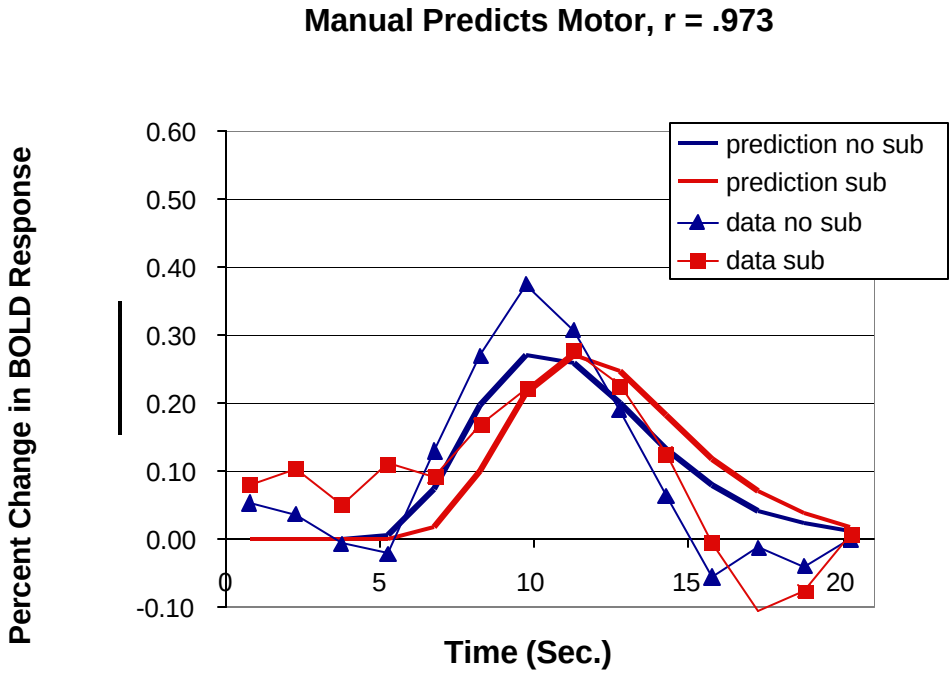

Figure 12

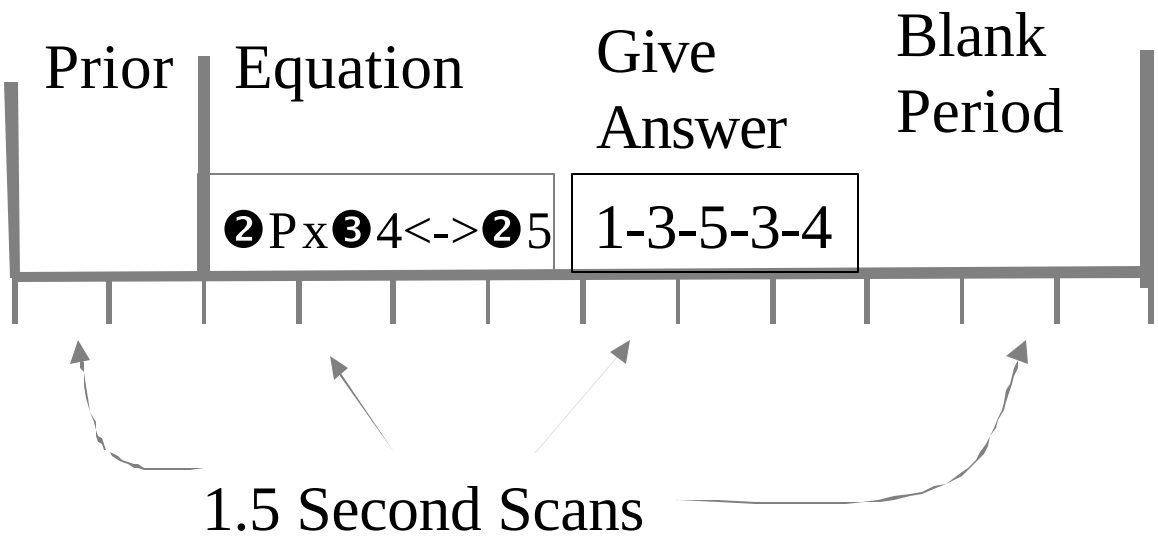
Prior
Equation
Give Answer
Blank Period
❷Px❸4<->❷5
1-3-5-3-4
1.5 Second Scans

Figure 13

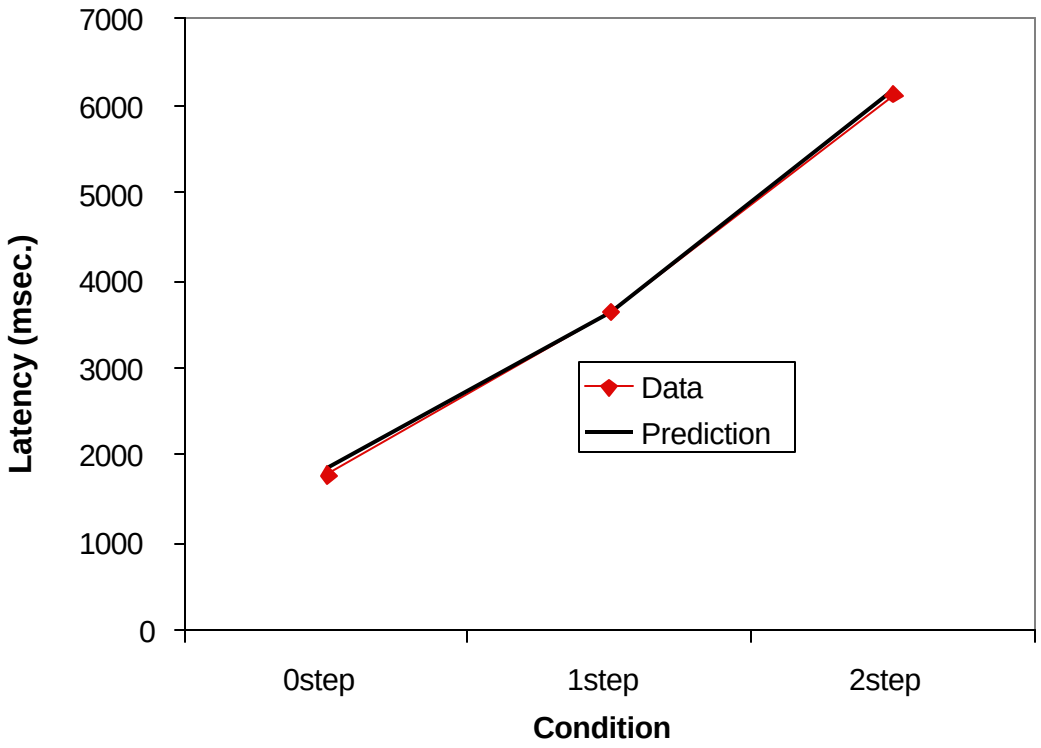
7000
6000
5000
4000
3000
2000
1000
0
Latency (msec.)
Data
Prediction
0step
1step
2step
Condition

Figure 14

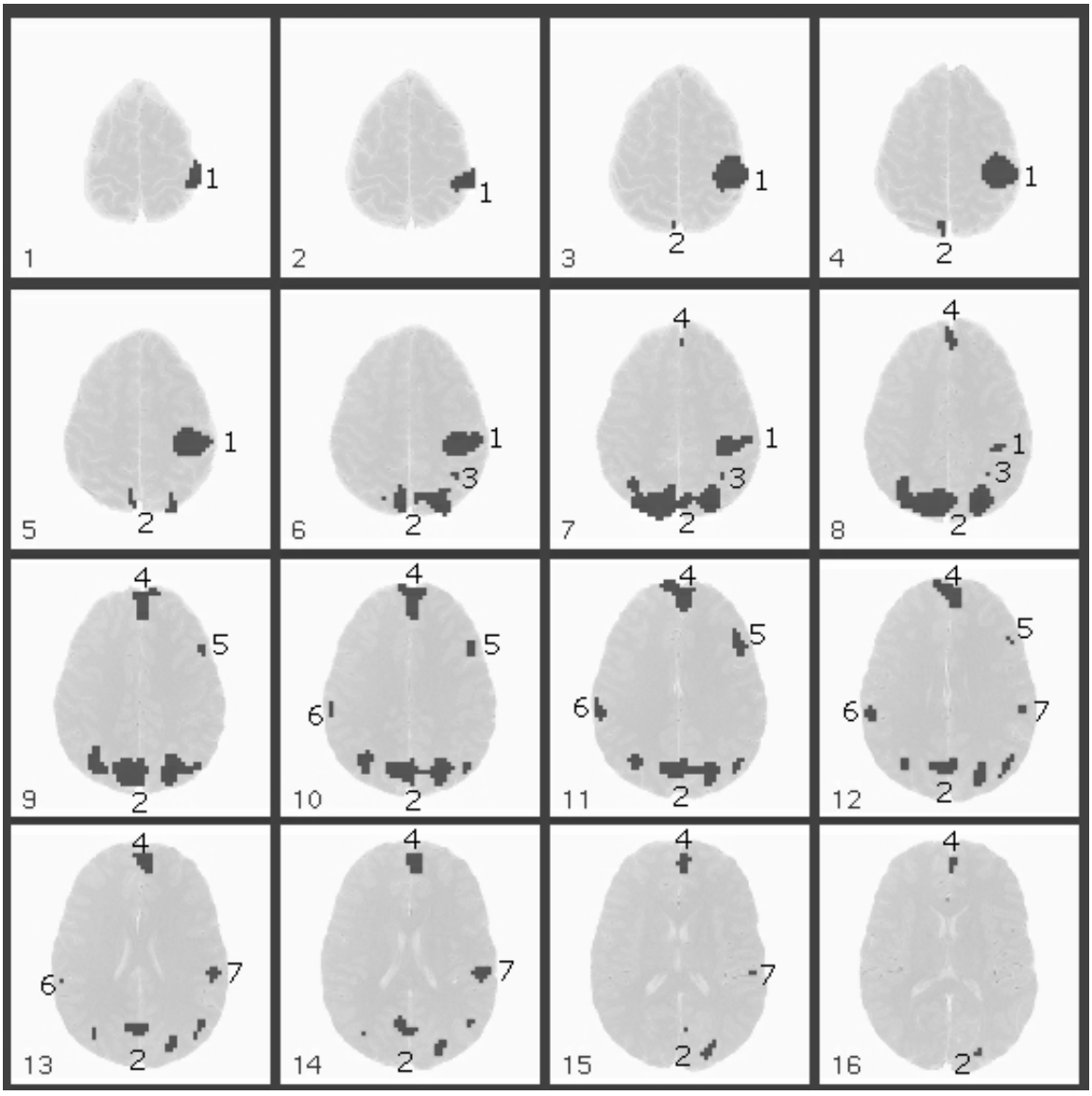

Figure 15

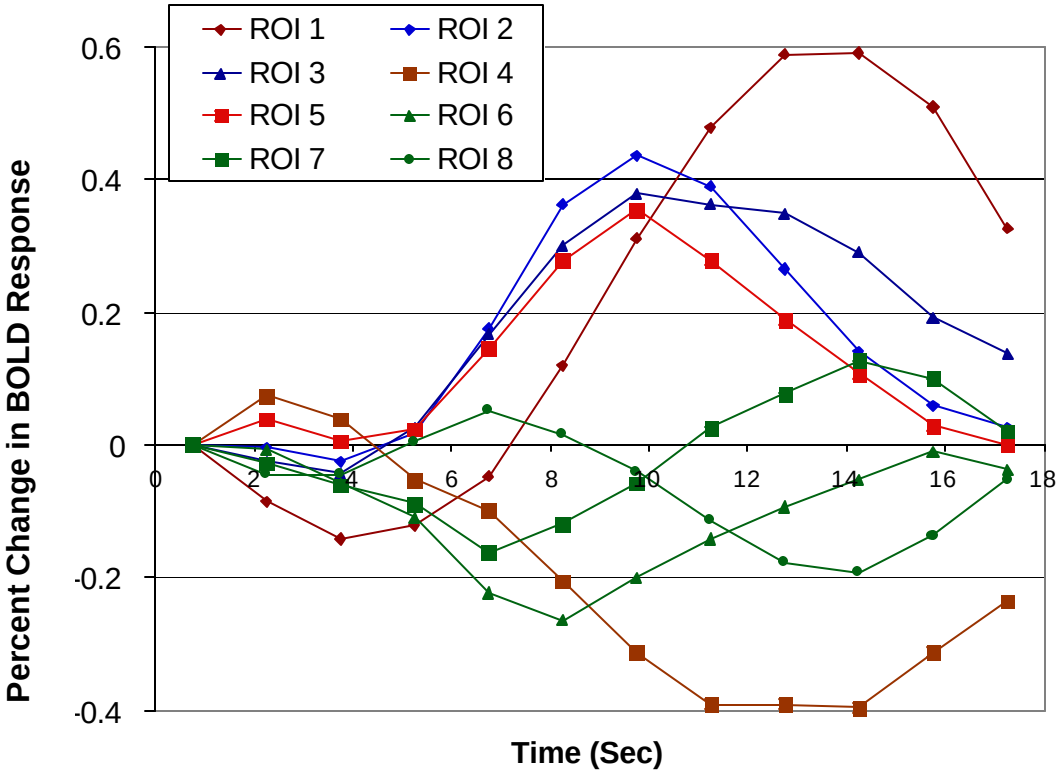
ROI 1
ROI 2
ROI 3
ROI 4
ROI 5
ROI 6
ROI 7
ROI 8
0.6
0.4
0.2
0
-0.2
-0.4
0
2
4
6
8
10
12
14
16
18
Percent Change in BOLD Response
Time (Sec)

Figure 16a

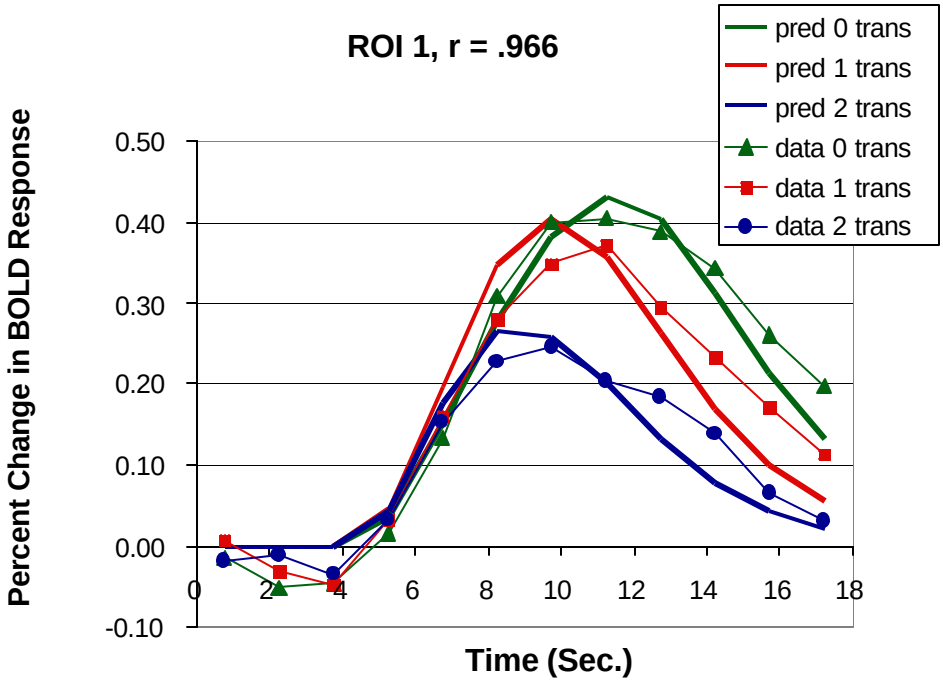

Figure 16b

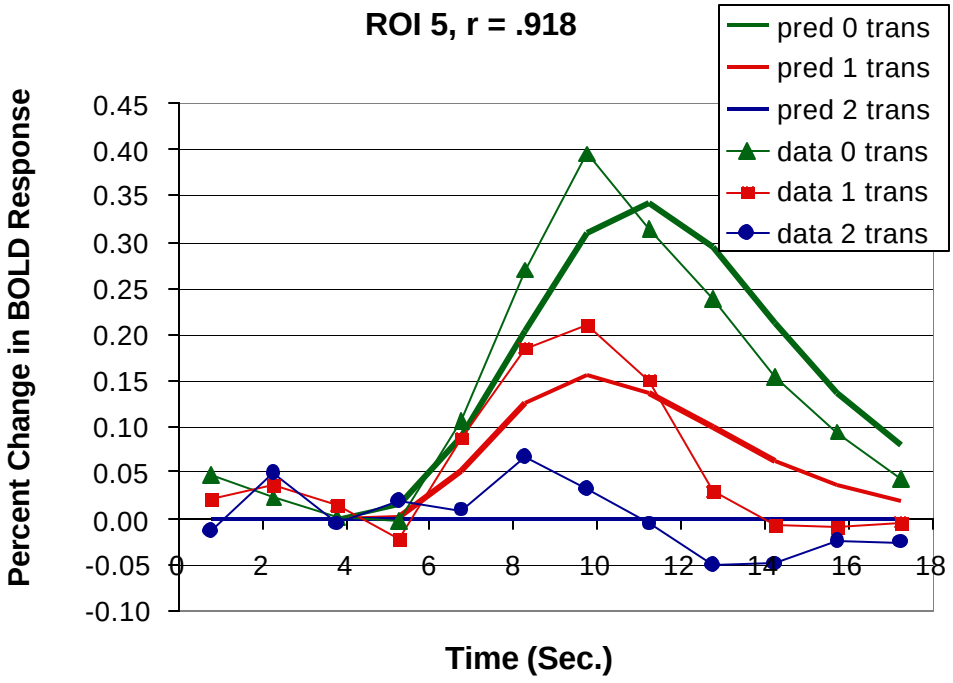

Figure 16c

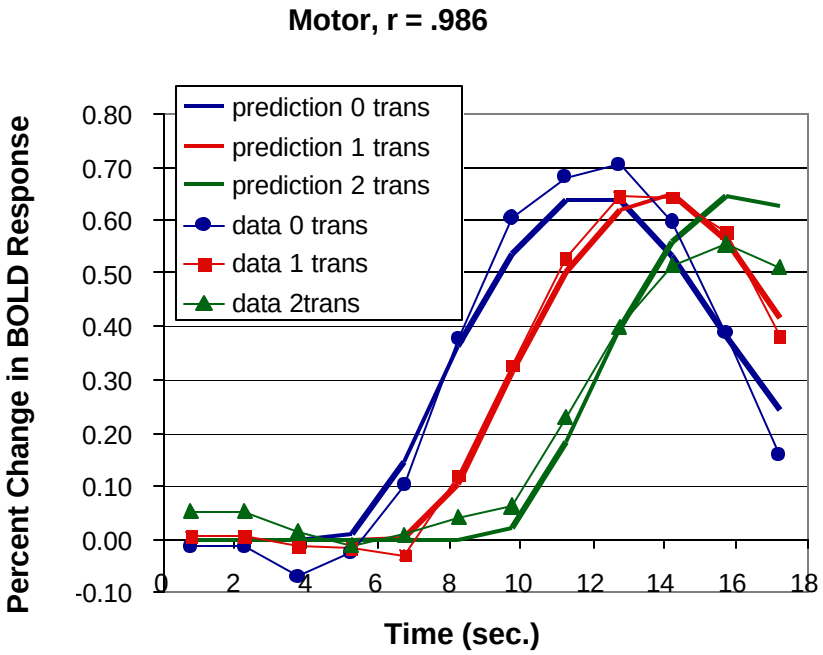
Motor, r = .986
prediction 0 trans
prediction 1 trans
prediction 2 trans
data 0 trans
data 1 trans
data 2trans
Percent Change in BOLD Response
0.80
0.70
0.60
0.50
0.40
0.30
0.20
0.10
0.00
-0.10
0
2
4
6
8
10
12
14
16
18
Time (sec.)

Figure 17

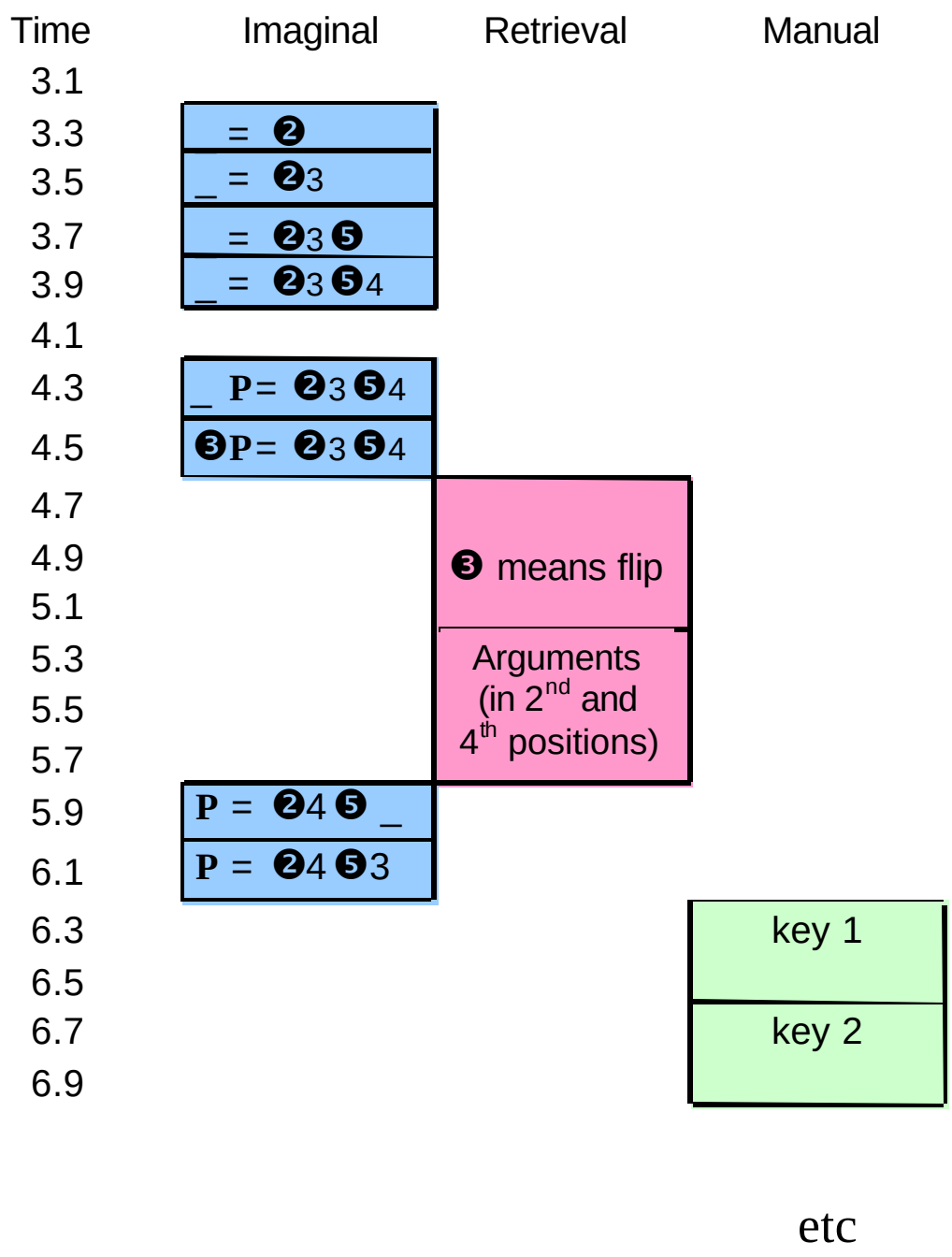
Time
Imaginal
Retrieval
Manual
3.1
3.3
3.5
3.7
3.9
4.1
4.3
4.5
4.7
4.9
5.1
5.3
5.5
5.7
5.9
6.1
6.3
6.5
6.7
6.9
= ❷
_ = ❷3
= ❷3 ❺
_ = ❷3 ❺4
_ P= ❷3 ❺4
❸P= ❷3 ❺4
❸ means flip
Arguments (in 2nd and 4th positions)
P = ❷4 ❺ _
P = ❷4 ❺3
key 1
key 2
etc

[1] The earlier Anderson et al studies were also concerned with an interaction between the size of the load and the physical complexity of the equation. This is an issue that we will not be pursuing here.

[2] (http://kraepelin.wpic.pitt.edu/his/index.html)

[3] An ACT-R model for a learning version of this task is to be found in Blessing (dissertation).

[4] ROI 8 is a small particle occurring in slices 18-20, not shown in the figure.